

IOWA STATE UNIVERSITY

Electrical and computer engineering

# Measurement-Based Hierarchical Framework for Time-Varying Stochastic Load Modeling

Project team: Argonne National Laboratory, NREL, Iowa State University, SIEMENS PTI

Dr. Zhaoyu Wang

Harpole-Pentair Assistant Professor

Iowa State University

# Overview

- Mathematical representation of WECC composite load model
- Dynamic order reduction of WECC composite load model
- Robust Time Varying Parameter Identification for Composite Loads
- SVM-Based Parameter Identification for Composite ZIP and Electronic Load Modeling

## Project Description

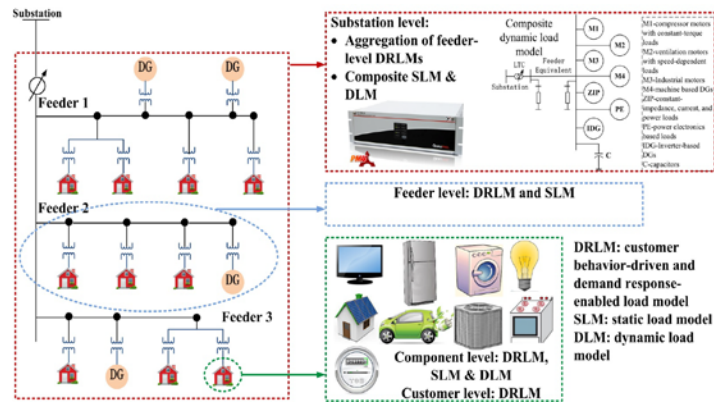
This project, led by ANL, is to develop a hierarchical load modeling structure to build time-varying, stochastic, customer behavior-driven and DR-enabled load models by leveraging practical utility data and laboratory experiments. The load modeling techniques leverage practical AMI, SCADA and PMU data at component, customer, feeder and substation levels.

## Expected Outcomes

- Static and dynamic load models at component, customer, feeder and substation levels, which are generic and applicable to various practical systems.
- Customer behavior-driven and demand response-enabled load models at component, customer, feeder and substation levels, which are generic and applicable to various practical systems.
- Load model identification techniques which are robust to measurement noises and bad data and suitable for on-line identification of model parameters.
- Recommendations on typical load model parameter values, ranges and probabilistic distributions.
- A set of commercially available software tools with developed load models, which include PSS/E at transmission level, CYME at distribution level, and RTDS/OPAL-RT at customer and component levels
- Technical reports and journal papers with detailed descriptions of load models, assumptions/limitations, laboratory/utility data tests, demonstrations with commercially-available software tools.

## Publications

- [1] A. Arif, Z. Wang, J. Wang, B. Mather, H. Bashualdo, and D. Zhao, "Load Modeling - A Review," *IEEE Transactions on Smart Grid*, vol. 9, no. 6, pp. 5986-5999, November 2018.
- [2] C. Wang, Z. Wang, J. Wang, and D. Zhao, "Robust Time-Varying Parameter Identification for Composite Load Modeling," *IEEE Transactions on Smart Grid*, accepted for publication.
- [3] C. Wang, Z. Wang, J. Wang, and D. Zhao, "SVM-Based Parameter Identification for Composite ZIP and Electronic Load Modeling," *IEEE Transactions on Power Systems*, accepted for publication.
- [4] J. Zhao, Z. Wang, and J. Wang, "Robust Time-Varying Load Modeling for Conservation Voltage Reduction Assessment," *IEEE Transactions on Smart Grid*, vol. 9, no. 4, pp. 3304-3312, July 2018.
- [5] Z. Ma, J. Xie, Z. Wang, "Mathematical representation of the WECC composite load model", arXiv preprint arXiv:1902.08866, Feb 2019.



Hierarchical load modeling framework

## Milestones

#	Milestone Name/Description	End Date
1	Overview of power system load modeling/industry practice, and Data Collection.	Month 6
2	Development and testing of load model identification algorithms with trained and validated data-driven models for load composition identification.	Month 12
3	Development and validation of load models at Component, Customer, and Feeder levels.	Month 18
4	Development and validation of load models at substation level.	Month 21
5	Typical ranges and time-varying probabilistic distributions of load models provided.	Month 24
6	Integration of developed load models to existing power system analysis tools with quantification of the operational benefits using the developed load/DG models	Month 30
7	Final reports documenting all models developed with examples of practical operation.	Month 36

- **Mathematical representation of WECC composite load model**
- Dynamic order reduction of WECC composite load model
- Robust Time Varying Parameter Identification for Composite Loads
- SVM-Based Parameter Identification for Composite ZIP and Electronic Load Modeling

# Motivation and approaches

- **Why mathematical representation is important to both research and engineering?**
  - Parameter identification
  - Sensitivity analysis
  - Dynamic order reduction
  - Dynamic behavior analysis
  - Simulation
- **Do we already have it?**
  - Commercial software has, but not accessible
  - PNNL's GridPack<sup>[9]</sup> has some parts, e.g., three-phase motor model
- **Why dynamic order reduction matters?**
  - Original WECC model has 166 parameters and 25 states
  - Computational burden in large-scale simulations
- Therefore, we will develop a *comprehensive* mathematical representation of *full* WECC composite load model. We will also reduce the model size using dynamic order reduction.

# WECC Composite Load Model (CMPLDWG)

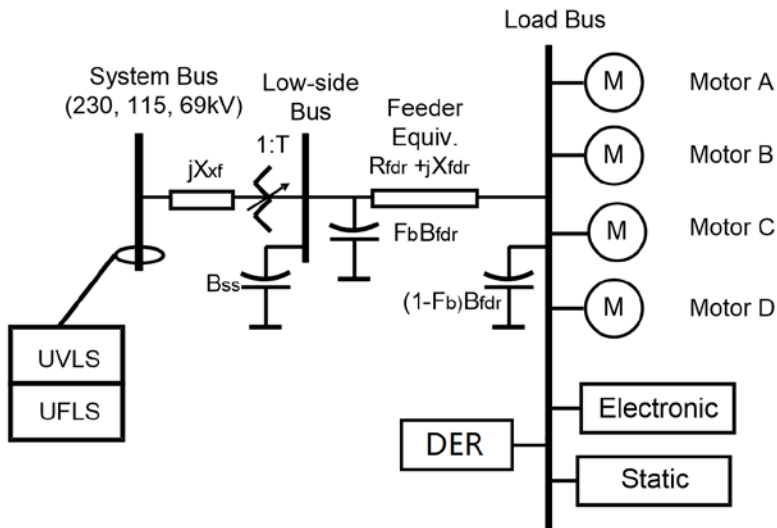


Fig. 1. The WECC CMPLDWG composite load model [3].

The CMPLDW model contains:

- 3 three-phase motors, A (chillers), B (fans), and C (pumps).
- 1 single-phase motor D (residential HVAC).
- 1 static ZIP load.
- 1 electronic load.
- A typical CMPLDW model has in total 121 parameters [4].
- DER\_A model has 45 parameters and 10 states [5].

CMPLDWG=CMPLDW+DG model (DER\_A)

# Three-phase motor model

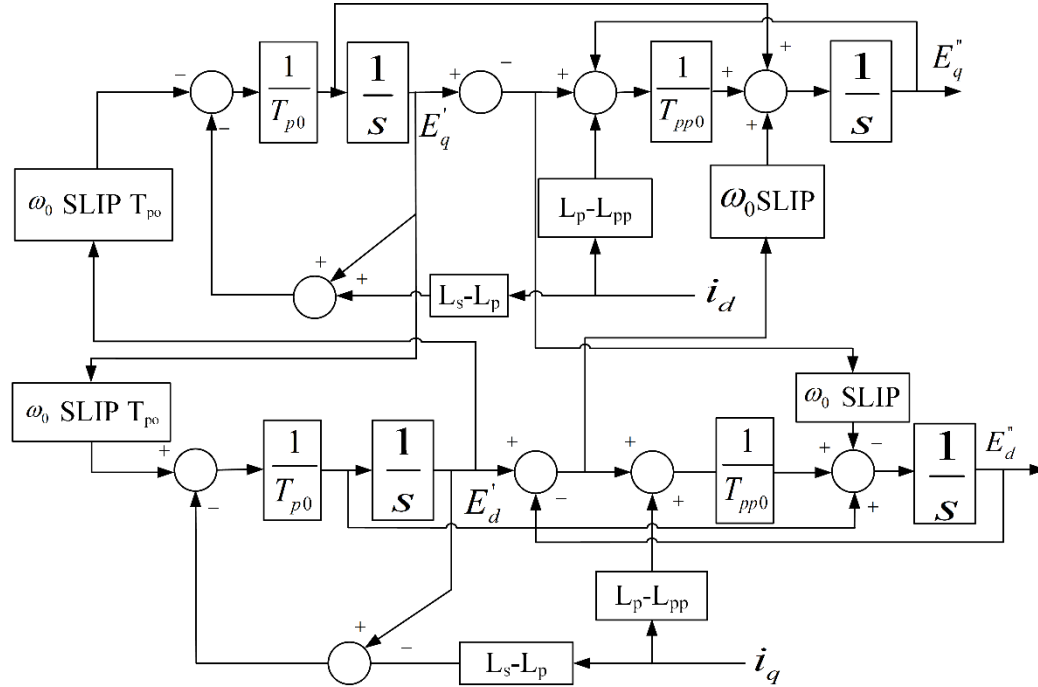


Fig. 2 The diagram of three-phase motor [3].

# Three-phase motor model

$$\dot{E}'_q = \frac{1}{T_{p0}} [-E'_q - i_d(L_s - L_p) - E'_d \cdot \omega_0 \cdot SLIP \cdot T_{p0}] \quad (1)$$

$$\dot{E}'_d = \frac{1}{T_{p0}} [-E'_d + i_q(L_s - L_p) + E'_q \cdot \omega_0 \cdot SLIP \cdot T_{p0}] \quad (2)$$

$$\dot{E}''_d = \frac{T_{p0} - T_{pp0}}{T_{p0}T_{pp0}} E'_d + \frac{T_{pp0}(L_s - L_p) + T_{p0}(L_p - L_{pp})}{T_{p0}T_{pp0}} i_q - \frac{1}{T_{pp0}} E''_d + \omega_0 \cdot SLIP \cdot E''_q \quad (3)$$

$$\dot{E}''_q = \frac{T_{p0} - T_{pp0}}{T_{p0}T_{pp0}} E'_q - \frac{T_{pp0}(L_s - L_p) + T_{p0}(L_p - L_{pp})}{T_{p0}T_{pp0}} i_d - \frac{1}{T_{pp0}} E''_q - \omega_0 \cdot SLIP \cdot E''_d \quad (4)$$

Electrical model  
(from Fig. 2).  
It is also the same  
as the model in  
[GridPACK v3.2](#).

**Fifth-order  
in total**

$$SLIP = -\frac{p \cdot E''_d \cdot i_d + q \cdot E''_q \cdot i_q - TL}{2H} \quad (5)$$

$$TL = T_{m0}(Aw^2 + Bw + C_0 + Dw^{Etrq}) \quad (6)$$

$$T_m = T_{m0} \cdot \omega^{Etrq} \quad (7)$$

$$w = 1 - SLIP \quad (8)$$

Mechanical model

where  $A, B, C_0, D, p, q$  and  $Etrq$  are parameters.



# Three-phase motor model

Other static equations are as follows:

$$i_d = \frac{r_s}{r_s^2 + L_{pp}^2} (V_d + E_d'') + \frac{L_{pp}}{r_s^2 + L_{pp}^2} (V_q + E_q'') \quad (9)$$

$$i_q = \frac{r_s}{r_s^2 + L_{pp}^2} (V_q + E_q'') - \frac{L_{pp}}{r_s^2 + L_{pp}^2} (V_d + E_d'') \quad (10)$$

$$V_d = \text{real}(V_t) \quad (11)$$

$$V_q = \text{imag}(V_t) \quad (12)$$

$$P = V_d i_d + V_q i_q \quad (13)$$

$$Q = V_d i_q - V_q i_d \quad (14)$$

# Single-phase motor model

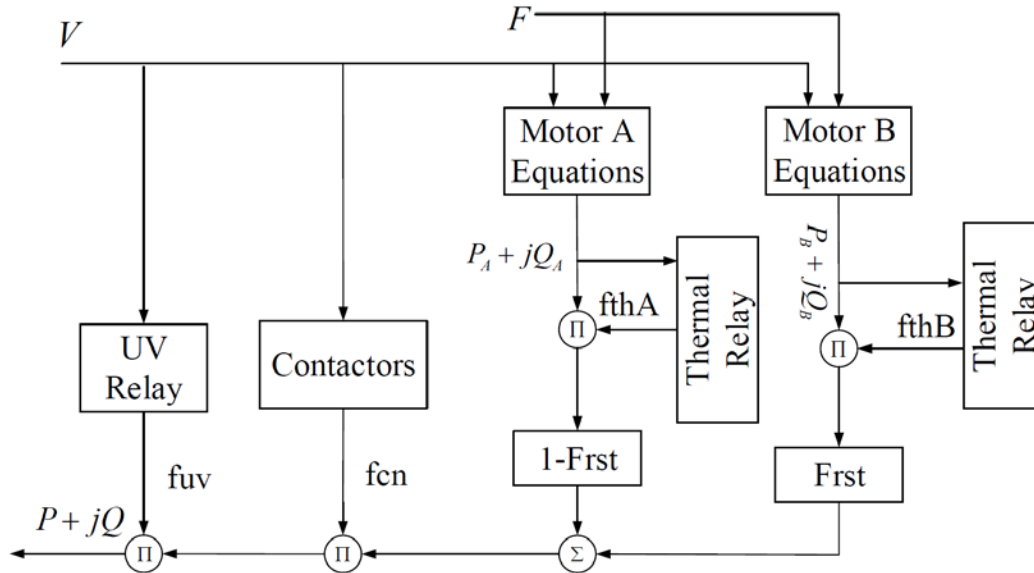


Fig. 3 The diagram of single-phase motor [3].

The single-phase AC motor is constructed as a performance model. Therefore, there is no need to derive its mathematical representation.

# DER\_A model diagram

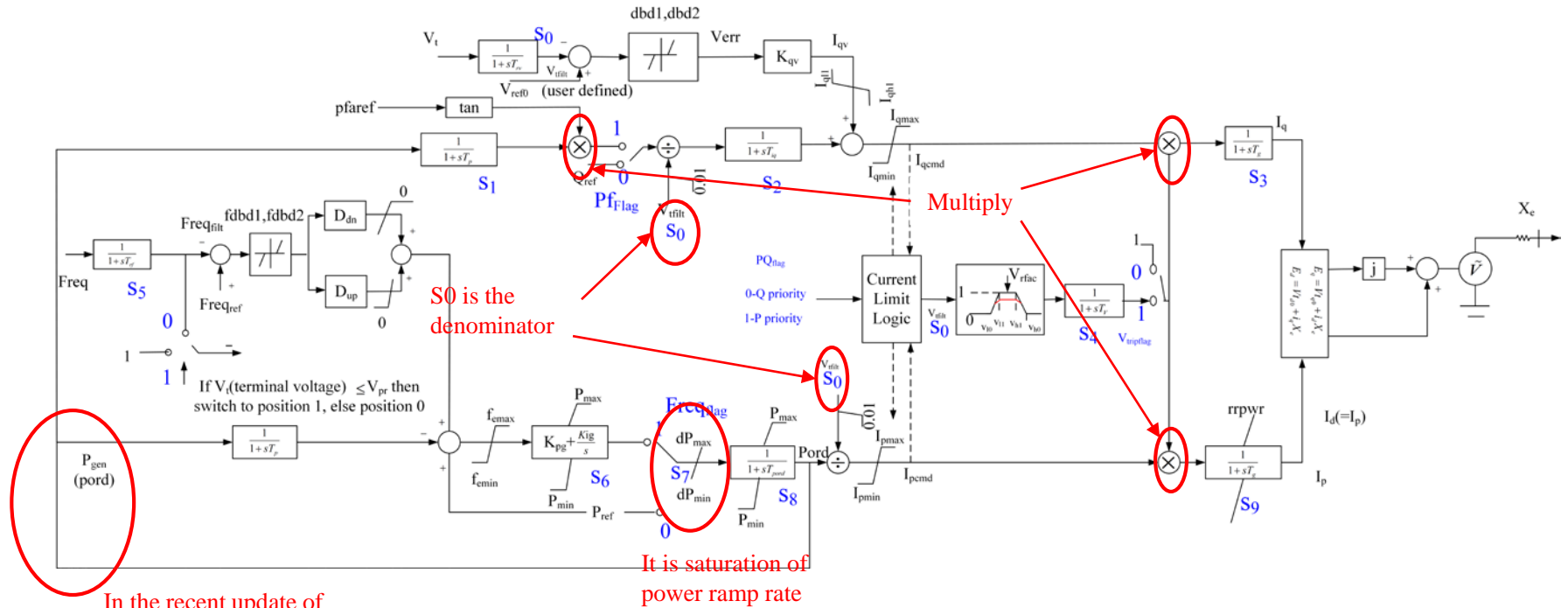
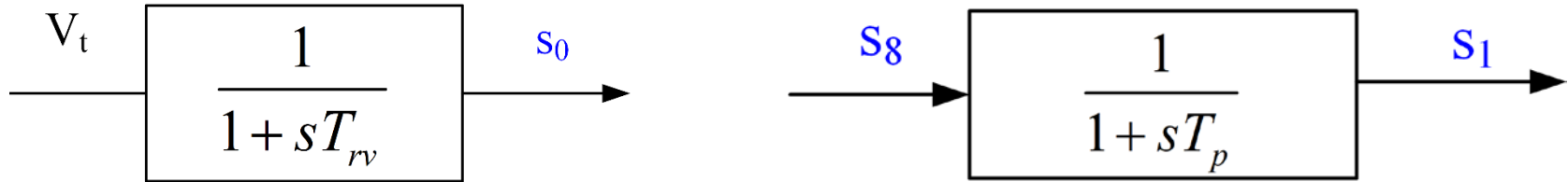


Fig. 4 The diagram of DER\_A model [5].

In the recent update of DER\_A model,  $P_{gen}$  is the feedback of  $P_{ord}$

# Mathematical Model of DER\_A



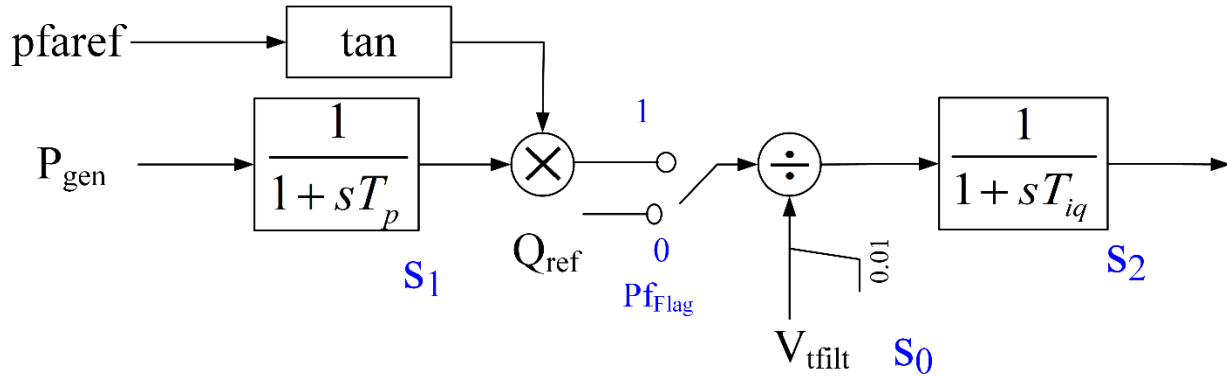
Equations of  $S_0$

$$\dot{S}_0 = \frac{1}{T_{rv}} (V_t - S_0) \quad (15)$$

Equations of  $S_1$

$$\dot{S}_1 = \frac{1}{T_p} (S_8 - S_1) \quad (16)$$

# Mathematical Model of DER\_A

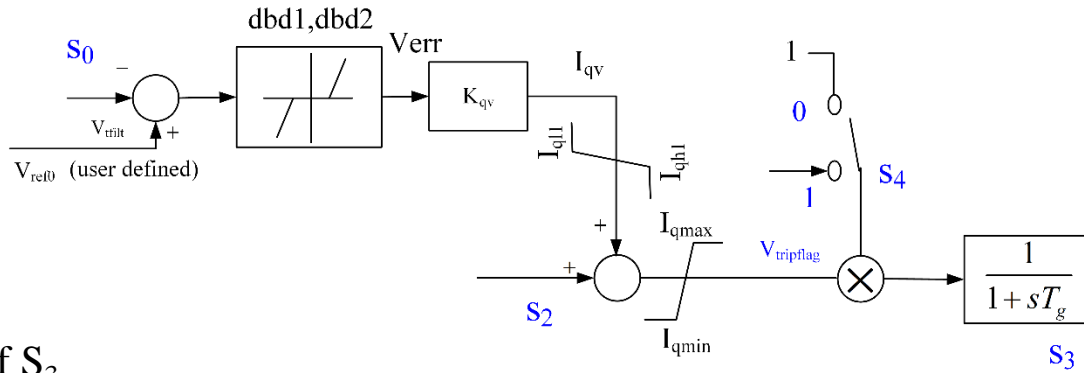


Equations of  $S_2$

$$\dot{S}_2 = \begin{cases} -\frac{S_2}{T_{iq}} + \frac{Q_{ref}}{T_{iq} \text{sat}_1(S_0)} & \text{if } P_{fFlag} = 0 \\ -\frac{S_2}{T_{iq}} + \frac{\tan(pf_{ref}) \times S_1}{T_{iq} \text{sat}_1(S_0)} & \text{if } P_{fFlag} = 1 \end{cases} \quad (17)$$

$$\text{sat}_1(x) = \begin{cases} x & \text{if } x \geq 0.01 \\ 0.01 & \text{if } x \leq 0.01 \end{cases} \quad (18)$$

# Mathematical Model of DER\_A



Equations of  $S_3$

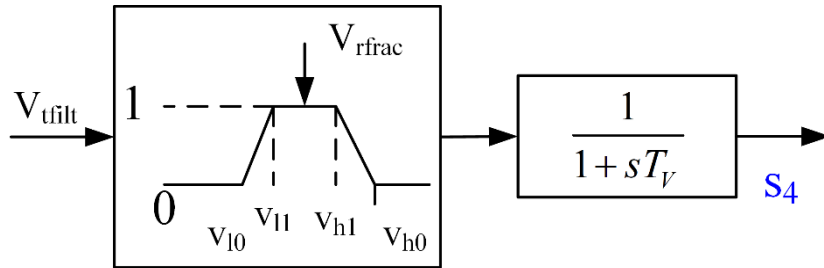
$$\dot{S}_3 = \begin{cases} \frac{S_3 - \text{sat}_2(S_2 + \text{sat}_3(DB_V(V_{ref0} - S_0) \cdot K_{qv}))}{T_g} & \text{if } V_{tripFlag} = 0 \\ \frac{S_3 - \text{sat}_2(S_2 + \text{sat}_3(DB_V(V_{ref0} - S_0) \cdot K_{qv})) \times S_4}{T_g} & \text{if } V_{tripFlag} = 1 \end{cases} \quad (19)$$

$$\text{sat}_2(x) = \begin{cases} I_{qmax} & \text{if } x \geq I_{qmax} \\ x & \text{if } I_{qmin} \leq x \leq I_{qmax} \\ I_{qmin} & \text{if } x \leq I_{qmin} \end{cases} \quad (21)$$

$$DB_V(x) = \begin{cases} x - dbd1 & \text{if } x > dbd1 \\ 0 & \text{if } dbd2 \leq x \leq dbd1 \\ x - dbd2 & \text{if } x < dbd2 \end{cases} \quad (20)$$

$$\text{sat}_3(x) = \begin{cases} I_{qh1} & \text{if } x \geq I_{qh1} \\ x & \text{if } I_{ql1} \leq x \leq I_{qh1} \\ I_{ql1} & \text{if } x \leq I_{ql1} \end{cases} \quad (22)$$

# Mathematical Model of DER\_A



Equations of  $S_4$

$$\dot{S}_4 = \frac{1}{T_v} (\text{VoltageProtection}(S_0, V_{rfrac}) - S_4) \quad (23)$$

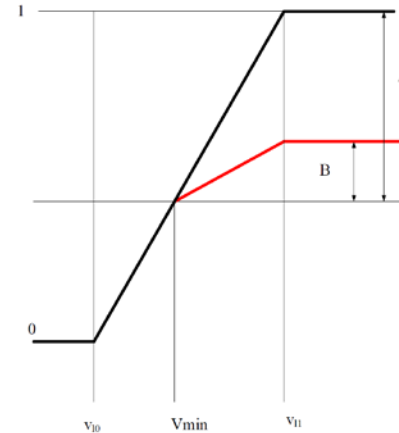


Fig. 5 The effect of  $V_{rfrac}$  [4].

$$B = V_{rfrac} \times A = V_{rfrac} \left( \frac{v_{l1} - V_{min}}{v_{l1} - v_{l0}} \right) \quad (24)$$

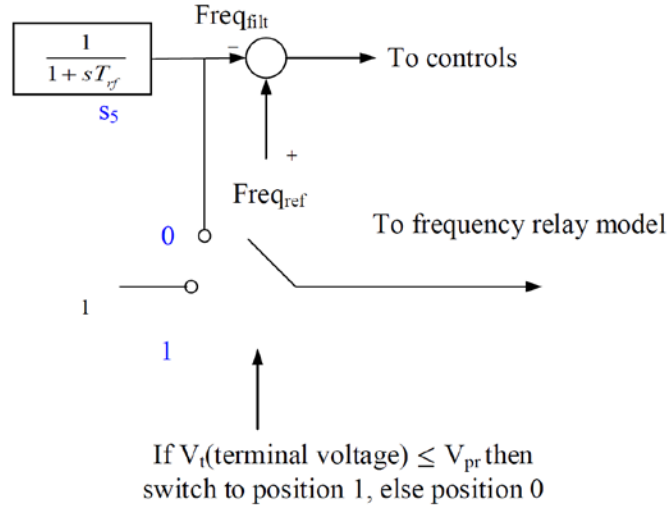
$V_{min}$  is the minimum value of  $V_t$  (from the diagram, it should be  $V_{t\_filt}$ )

# Mathematical Model of DER\_A

$$\text{VoltageProtection}(S_0, V_{rfrac}) = \begin{cases} \frac{V_t - V_{l0}}{V_{l1} - V_{l0}} & \text{if } V_{l0} \leq V_t \leq V_{\min} \\ \frac{V_t - V_{l0}}{V_{l1} - V_{l0}} & \text{if } V_{\min} \leq V_t \leq V_{l1} \text{ and the voltage stays below } V_{l1} \text{ for a duration less than } t_{lv1} \\ 1 & \text{if } V_{l1} < V_t < V_{h1} \text{ and the voltage stays below } V_{h1} \text{ for a duration less than } t_{lv1} \\ \frac{V_{h0} - V_t}{V_{h0} - V_{h1}} & \text{if } V_{h1} \leq V_t \leq V_{h0} \text{ and the voltage stays over } V_{h1} \text{ for a duration less than } t_{hv1} \\ V_{rfrac} \frac{V_t - V_{\min}}{V_{l1} - V_{l0}} & \text{if } V_{\min} \leq V_t \leq V_{l1} \text{ and the voltage stays below } V_{l1} \text{ for a duration greater than } t_{lv1} \\ V_{rfrac} \left( \frac{V_{l1} - V_{\min}}{V_{l1} - V_{l0}} \right) & \text{if } V_{l1} < V_t < V_{h1} \text{ and the voltage stays below } V_{h1} \text{ for a duration greater than } t_{lv1} \\ V_{rfrac} \left( \frac{V_{\max} - V_t}{V_{h0} - V_{h1}} \right) & \text{if } V_{h1} \leq V_t \leq V_{\max} \text{ and the voltage stays below } V_{l1} \text{ for a duration greater than } t_{hv1} \\ \frac{V_{h0} - V_t}{V_{h0} - V_{h1}} & \text{if } V_{\max} \leq V_t \leq V_{h0} \\ 0 & \text{otherwise} \end{cases} \quad (25)$$



# Mathematical Model of DER\_A



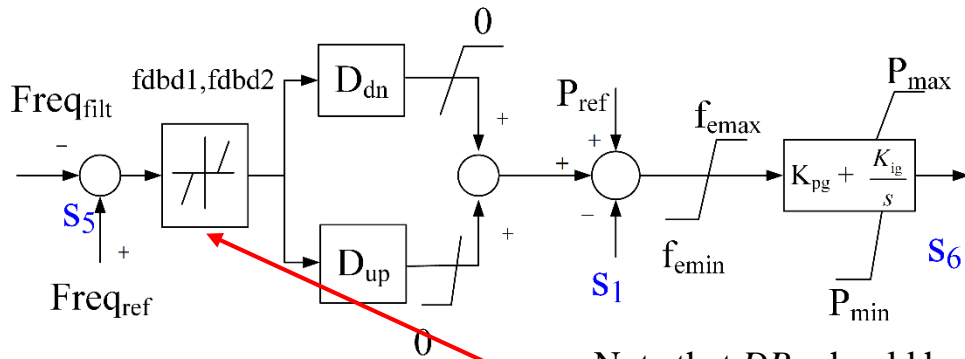
Equations of  $S_5$

$$\dot{S}_5 = \frac{1}{T_{rf}} (Freq - S_5) \quad (26)$$

Frequency trip logic:

- If frequency goes below  $f_l$  for more than  $t_{fl}$  seconds, then the entire model will trip.
- If frequency goes above  $f_h$  for more than  $t_{fh}$  seconds, then the entire model will trip.

# Mathematical Model of DER\_A



$$sat_4(x) = \begin{cases} f_{emax} & \text{if } x \geq f_{emax} \\ x & \text{if } f_{emin} \leq x \leq f_{emax} \\ f_{emin} & \text{if } x \leq f_{emin} \end{cases} \quad (28)$$

$$sat_5(x) = \begin{cases} x & \text{if } x \leq 0 \\ 0 & \text{if } x > 0 \end{cases} \quad (29)$$

$$sat_6(x) = \begin{cases} x & \text{if } x > 0 \\ 0 & \text{if } x \leq 0 \end{cases} \quad (30)$$

Note that  $DB_F$  should have the same structure as  $DB_V$ .

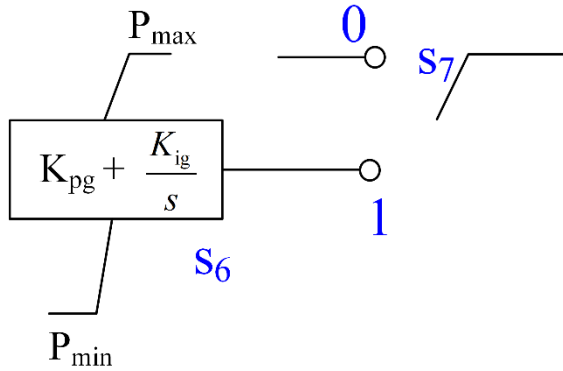
Equations of  $S_6$

$$\begin{aligned} \dot{S}_6 = & K_{ig} sat_4(P_{ref} - S_1 + sat_5[D_{dn} \cdot DB_F(Freq_{ref} - S_5)]) \\ & + sat_6[D_{up} \cdot DB_F(Freq_{ref} - S_5)]) + \frac{K_{pg}}{T_p} S_1 \\ & + G_{dn}(Freq - S_5) + G_{up}(Freq - S_5) - \frac{K_{pg} S_8}{T_p} \end{aligned} \quad (27)$$

$$G_{dn}(x) = \begin{cases} -K_{pq} D_{dn} x / T_{rf} & \text{if } x < fdbd1 \text{ or } x > fdbd2, \\ & \text{and } D_{dn} x / T_{rf} \geq 0 \\ 0 & \text{otherwise} \end{cases} \quad (31)$$

$$G_{up}(x) = \begin{cases} -K_{pq} D_{up} x / T_{rf} & \text{if } x < fdbd1 \text{ or } x > fdbd2, \\ & \text{and } D_{up} x / T_{rf} < 0 \\ 0 & \text{otherwise} \end{cases} \quad (32)$$

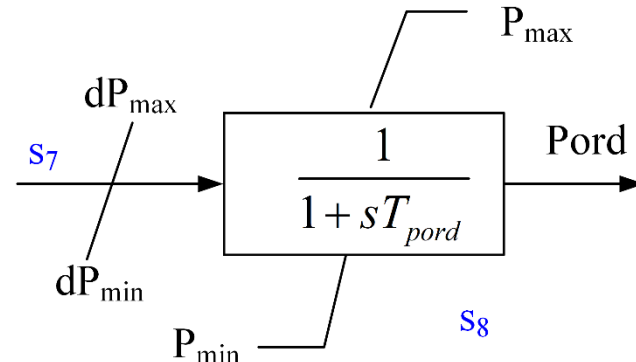
# Mathematical Model of DER\_A



Equations of  $S_7$

$$\dot{S}_7 = \begin{cases} 0 & \text{if } Freq_{flag} = 0 \\ sat_8(sat_7(S_6)) & \text{if } Freq_{flag} = 1 \end{cases} \quad (33)$$

$$sat_7(x) = \begin{cases} P_{max} & \text{if } x \geq P_{max} \\ x & \text{if } P_{min} \leq x \leq P_{max} \\ P_{min} & \text{if } x \leq P_{min} \end{cases} \quad (34)$$

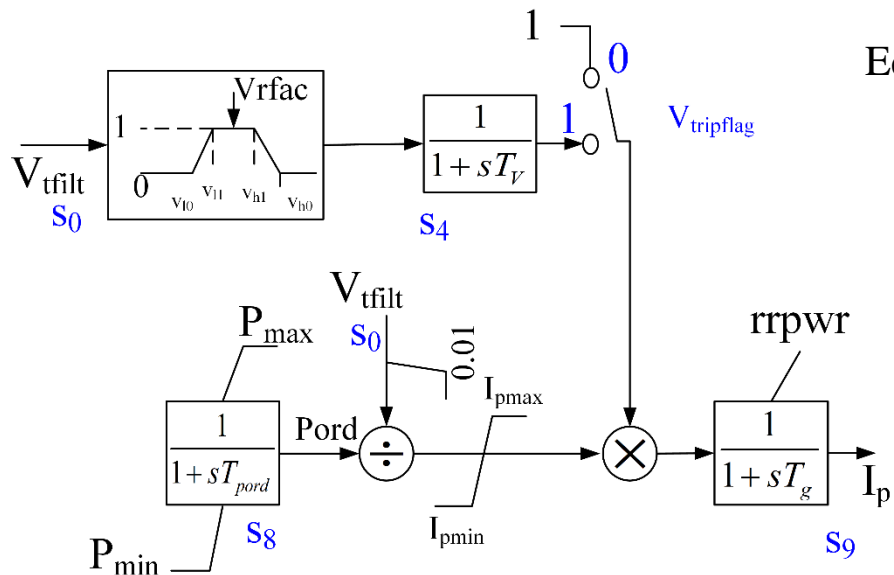


Equations of  $S_8$

$$\dot{S}_8 = \frac{1}{T_{pord}} (S_7 - S_8) \quad (35)$$

$$sat_8(x) = \begin{cases} dP_{max} & \text{if } x \geq dP_{max} \\ x & \text{if } dP_{min} \leq x \leq dP_{max} \\ dP_{min} & \text{if } x \leq dP_{min} \end{cases} \quad (36)$$

# Mathematical Model of DER\_A



Equations of  $S_9$

$$\dot{S}_9 = \begin{cases} \frac{1}{T_g} \left( \text{sat}_9 \left( \frac{\text{sat}_7(S_8)}{\text{sat}_1(S_0)} \right) \times S_4 - S_9 \right) & \text{if } V_{tripflag} = 1 \\ \frac{1}{T_g} \left( \text{sat}_9 \left( \frac{\text{sat}_7(S_8)}{\text{sat}_1(S_0)} \right) - S_9 \right) & \text{if } V_{tripflag} = 0 \end{cases} \quad (37)$$

$$\text{sat}_9(x) = \begin{cases} I_{pmax} & \text{if } x \geq I_{pmax} \\ x & \text{if } I_{pmin} \leq x \leq I_{pmax} \\ I_{pmin} & \text{if } x \leq I_{pmin} \end{cases} \quad (38)$$

# Mathematical Model of DER\_A

$$\dot{S}_0 = \frac{1}{T_{rv}} (V_t - S_0)$$

$$\dot{S}_1 = \frac{1}{T_p} (S_8 - S_1)$$

$$\dot{S}_2 = \begin{cases} -\frac{S_2}{T_{iq}} + \frac{Q_{ref}}{T_{iq} \text{sat}_1(S_0)} & \text{if } P_{fFlag} = 0 \\ -\frac{S_2}{T_{iq}} + \frac{\tan(\text{pfaref}) \times S_1}{T_{iq} \text{sat}_1(S_0)} & \text{if } P_{fFlag} = 1 \end{cases}$$

$$\dot{S}_3 = \begin{cases} -\frac{S_3 - \text{sat}_2(S_2 + \text{sat}_3(DB_V(V_{ref0} - S_0) \cdot K_{qv}))}{T_g} & \text{if } V_{tripFlag} = 0 \\ -\frac{S_3 - \text{sat}_2(S_2 + \text{sat}_3(DB_V(V_{ref0} - S_0) \cdot K_{qv})) \times S_4}{T_g} & \text{if } V_{tripFlag} = 1 \end{cases}$$

$$\dot{S}_4 = \frac{1}{T_v} (\text{VoltageProtection}(S_0, V_{rfrac}) - S_4)$$

$$\dot{S}_5 = \frac{1}{T_{rf}} (\text{Freq} - S_5)$$

$$\begin{aligned} \dot{S}_6 = & K_{ig} \text{sat}_4(P_{ref} - S_1 + \text{sat}_5[D_{dn} \cdot DB_F(\text{Freq}_{ref} - S_5)]) \\ & + \text{sat}_6[D_{up} \cdot DB_F(\text{Freq}_{ref} - S_5)] + \frac{K_{pg}}{T_p} S_1 \\ & + G_{dn}(\text{Freq} - S_5) + G_{up}(\text{Freq} - S_5) - \frac{K_{pg} S_8}{T_p} \end{aligned}$$

$$\dot{S}_7 = \begin{cases} 0 & \text{if } \text{Freq}_{flag} = 0 \\ \text{sat}_8(\text{sat}_7(S_6)) & \text{if } \text{Freq}_{flag} = 1 \end{cases}$$

$$\dot{S}_8 = \frac{1}{T_{pord}} (S_7 - S_8)$$

$$\dot{S}_9 = \begin{cases} \frac{1}{T_g} \left( \text{sat}_9 \left( \frac{\text{sat}_7(S_8)}{\text{sat}_1(S_0)} \right) \times S_4 - S_9 \right) & \text{if } V_{tripflag} = 1 \\ \frac{1}{T_g} \left( \text{sat}_9 \left( \frac{\text{sat}_7(S_8)}{\text{sat}_1(S_0)} \right) - S_9 \right) & \text{if } V_{tripflag} = 0 \end{cases}$$



# Simulation Setup (MATLAB)

- The simulation is conducted in four parts: Motor A, Motor B, Motor C and DER\_A.
- We use the method in [5] to generate the input voltage, and the frequency is set to be 60 HZ.

$$V(t) = \begin{cases} a, & \text{if } 1 \leq t \leq (1 + (b/60)) \\ -\frac{-(1-d)}{(b/60) - c} & \text{for } (1 + (b/60)) \leq t \leq 1 + c, \text{ and} \\ 1, & \text{otherwise} \end{cases} \quad (39)$$

# Simulation Setup (MATLAB)

Table I

Parameter setting of Motor A, B and C.

Motor A		Motor B		Motor C	
FmA	0.167	FmB	0.167	FmC	0.167
MtypA	3	MtypB	3	MtypC	3
LFmA	0.7	LFmB	0.8	LFmC	0.8
RsA	0.04	RsB	0.03	RsC	0.03
LsA	1.8	LsB	1.8	LsC	1.8
LpA	0.1	LpB	0.16	LpC	0.16
LppA	0.083	LppB	0.12	LppC	0.12
TpoA	0.092	TpoB	0.1	TpoC	0.1
TppoA	0.002	TppoB	0.0026	TppoC	0.0026
HA	0.05	HB	1	HC	0.1
EtrqA	0	EtrqB	2	EtrqC	2
Vtr1A	0.75	Vtr1B	0.5	Vtr1C	0.5
Ttr1A	$\infty$	Ttr1B	0.02	Ttr1C	0.02
Ftr1A	0.2	Ftr1B	0.2	Ftr1C	0.2
Vrc1A	0.9	Vrc1B	0.65	Vrc1C	0.65
Trc1A	$\infty$	Trc1B	0.6	Trc1C	0.6
Vtr2A	0.5	Vtr2B	0.7	Vtr2C	0.7
Ttr2A	0.02	Ttr2B	0.02	Ttr2C	0.02
Ftr2A	0.47	Ftr2B	0.3	Ftr2C	0.3
Vrc2A	0.639	Vrc2B	0.85	Vrc2C	0.85
Trc2A	0.73	Trc2B	$\infty$	Trc2C	$\infty$

Table II

Parameter setting of DER\_A [5].

Description	Units	Value	Description	Value
Trv	(s),	0.02	Pfflag; 1: constant power factor, 0: constant Q control	1
dbd1	(pu),	-0.05	FreqFlag; 1: frequency control enabled, 0: frequency control disabled	0
dbd2	(pu),	0.05	PQflag; 1: P priority for current limit, 0: Q-priority	0
Kqv	(pu/pu),	5	Genflag; 1: unit is a generator, 0: unit is a storage device (Note 6)	1
Vref0	(pu),	-1	Vtripflag (flag to enable/disable voltage trip logic); 1: enable, 0: disable	1
Tp	(s),	0.02	Ftripflag (flag to enable/disable frequency trip logic); 1: enable, 0: disable	1
Tiq	(s),	0.02	Kig	(pu), 10
Ddn	(pu),	0.05	lmax	(pu), 1.2
Dup	(pu),	0.05	vI0	(pu), 0.5
fdbd1	(pu),	-0.00028	vI1	(pu), 0.88
fdbd2	(pu),	0.000283	vh0	(pu), 1.2
femax	(pu),	99	vh1	(pu), 1.05
femin	(pu),	-99	tv0	(s), 0.05
PMAX	(pu),	1.1	tv1	(s), 2
PMIN	(pu),	0	tvh0	(s), 0.05
dPmax	(pu/s),	0.5	tvh1	(s), 2
dPmin	(pu/s),	-0.5	Vfrac	fraction 0.7
Tpord	(s),	0.02		
Kpg	(pu),	0.1	fl	(Hz), 59.93
			fh	(Hz), 60.07
			tfl	(s), 7.1
			tffh	(s), 7.1
			Tg	(s), 0.02
			rrpwr	(pu/s), 0.5
			Tv	(s), 0.02
			Xe	(pu), 0.2
			lqh1	(pu), 1.0
			lql1	(pu), -1.0
			Vpr	(pu), 0.8

# Simulation Results (MATLAB)

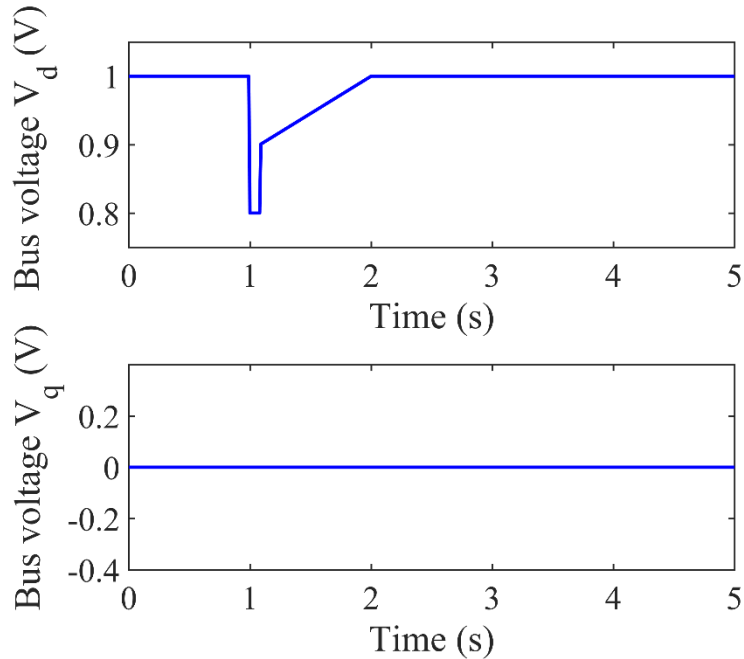


Fig. 6 Bus voltages of mathematical and PSS/E model of three-phase motor.

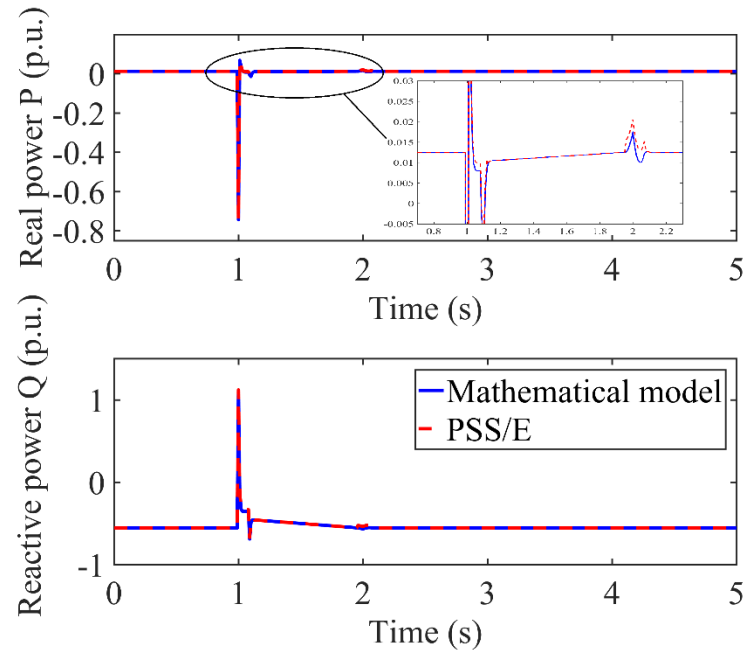


Fig. 7 Real and reactive power of mathematical and PSS/E model of three-phase motor A.



# Simulation Results (MATLAB)

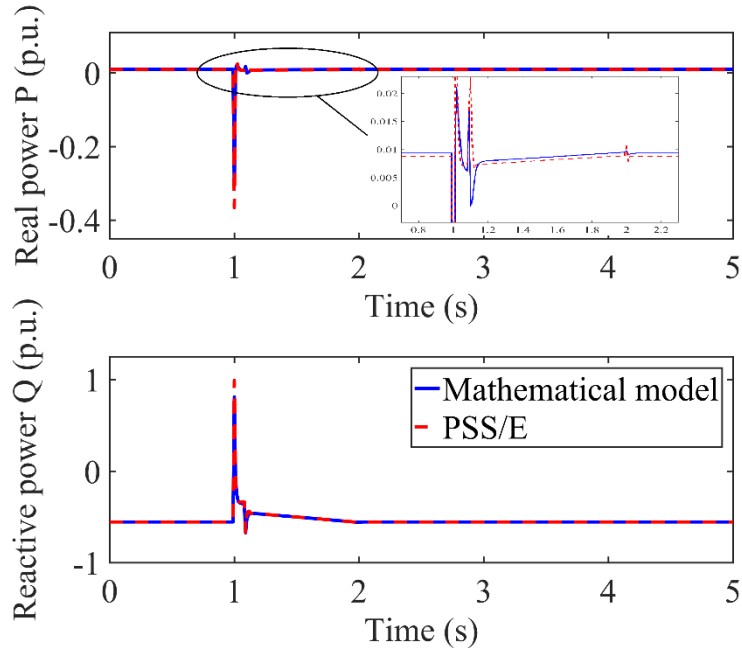


Fig. 8 Real and reactive power of mathematical and PSS/E model of three-phase motor B.

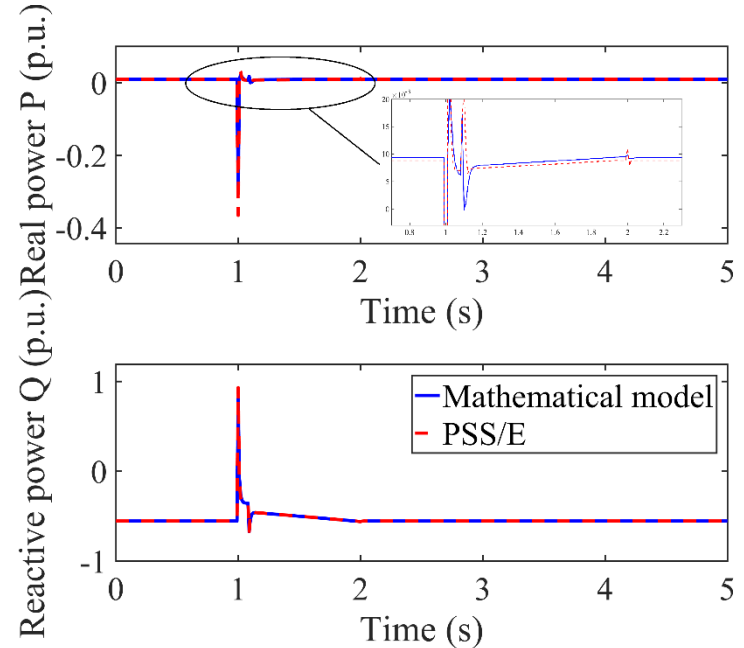


Fig. 9 Real and reactive power of mathematical and PSS/E model of three-phase motor C.

# Simulation Results (MATLAB)

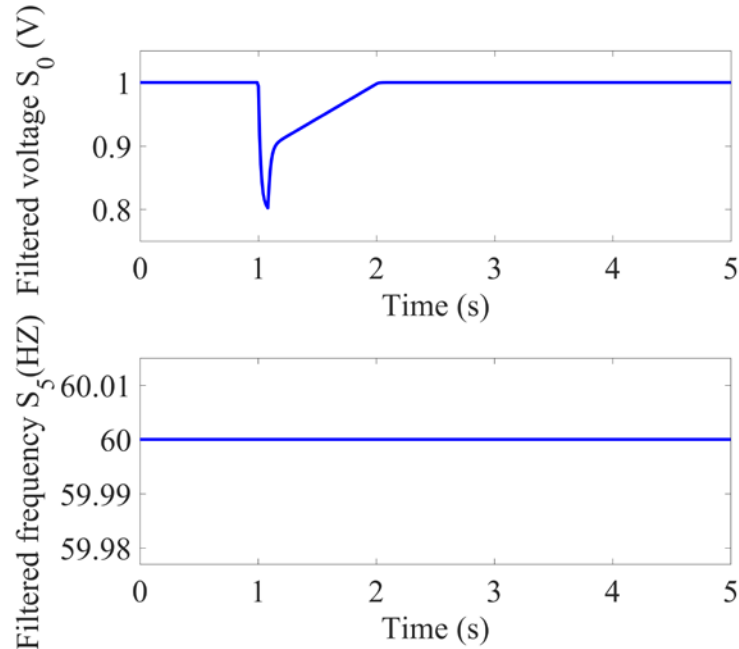


Fig. 10 Filtered input voltage and frequency of DER\_A (see Fig. 4 on slide 8).

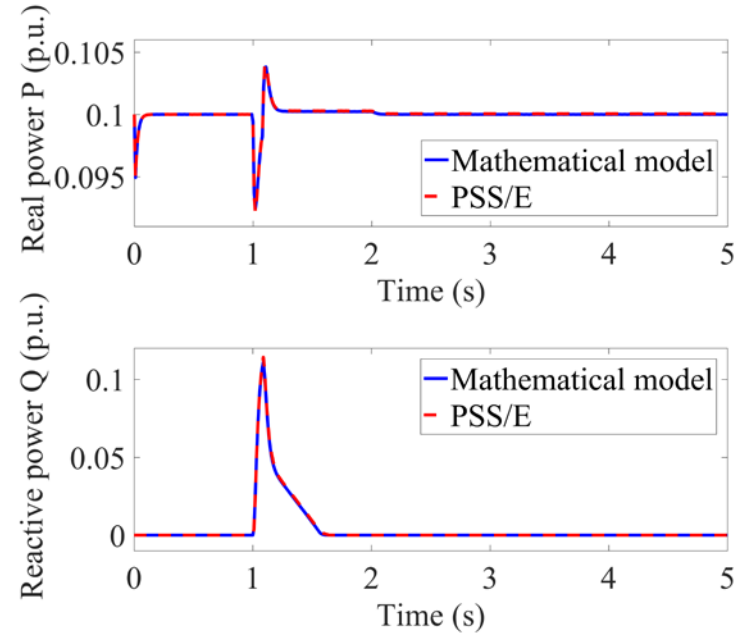


Fig. 11 Real and reactive power of mathematical and PSS/E model of DER\_A.

- Mathematical representation of WECC composite load model
- **Dynamic order reduction of WECC composite load model**
- Robust Time Varying Parameter Identification for Composite Loads
- SVM-Based Parameter Identification for Composite ZIP and Electronic Load Modeling

# Reduced-Order Large-Signal Model

- The existing WECC composite load model has more than 25 states (15 for three-phase motors, 10 for DER\_A and other components) and more than 160 parameters, which extremely increases the computation burden.
- The WECC model exhibits behaviors at two time-scales: faster dynamics and slower dynamics.
- We will propose a reduced-order large-signal model which has similar response to the original model.
- The reduced-order model will be developed based on singular perturbation theory that separates system states into fast and slow dynamics.

# Singular perturbation theory

Consider a singular perturbation model of a dynamical system whose derivatives of some of the states are multiplied by a small positive parameter  $\varepsilon$  (perturbation coefficient) as follows

$$\begin{aligned}\dot{x} &= F(x, z, u, t, \varepsilon) \\ \varepsilon \dot{z} &= G(x, z, u, t, \varepsilon)\end{aligned}\tag{40}$$

where  $x \in R^n$  representing slower dynamics,  $z \in R^m$  representing faster dynamics Let  $\varepsilon=0$ , we have

$$0 = G(x, z, u, t)\tag{41}$$

If  $G$  in (41) has at least one isolated real roots

$$z = h_i(x, u, t), i=1,2,\dots,k\tag{42}$$

Substitute (42) into (40), we obtain the reduced order model as follows

$$\dot{x} = F(x, h_i(x, u, t), u, t)\tag{43}$$

Note that the dimension of (40) is reduced from  $n+m$  to  $n$ .

Compared to conventional order reduction that simply ignores some dynamic states, our method uses slower dynamics to represent faster ones, thus reducing order while maintaining all dynamic characteristics.

# Singular perturbation theory

Even though we can get the reduced-order model using the above method, the accuracy of the reduced model is not guaranteed. Define a new time variable  $\tau = (t - t_0)/\varepsilon$ , and introduce the boundary-layer model as follows,

$$\frac{dy}{d\tau} = g(t, x, y + h(t, x), 0) \quad (44)$$

where  $y = z - h(t, x)$  is the change of state variables. If the system satisfies the following assumptions,

**Assumption 1:** On a compact subset of  $\Omega_x \times \Omega_y$ , functions  $f, g$  are  $\mathcal{C}^1$  and has bounded continuous first partial derivative with respect to  $t$ ;  $h$  and Jacobian  $\partial g/\partial z$  have bounded first partial derivatives;  $\partial f/\partial x$  is Lipschitz in  $x$  uniformly in  $t$ ;

**Assumption 2:** the origin of the reduced model (43) is a uniformly exponentially stable equilibrium and there is a Lyapunov function  $V(t, x)$  satisfying

$$W_1(x) \leq V(t, x) \leq W_2(x) \quad (45)$$

$$\frac{\partial V}{\partial t} + \frac{\partial V}{\partial x} f(t, x) \leq -W_3(x) \quad (46)$$

where  $W_i$  are continuous positive definite functions on  $\Omega_x$  and  $\{x | W_1(x) \leq c\}$  is a compact subset of  $\Omega_x$ ;

# Singular perturbation theory

**Assumption 3:** the origin of the boundary-layer model (44) is a uniformly exponentially stable equilibrium; Then by Tikhonov's theorem on the infinite time interval, there are compact sets  $\Omega_x, \Omega_y$  and positive constant  $\varepsilon^*$  and  $k_i$ , such that for all  $t_0 \geq 0, x(t_0) \in \Omega_x, y(t_0) \in \Omega_y$  and  $0 < \varepsilon < \varepsilon^*$ , the original system (40) has unique solutions  $x(t, \varepsilon)$  and  $z(t, \varepsilon)$  uniformly satisfying

$$\|x(t, \varepsilon) - \bar{x}(t)\| \leq k_1 \varepsilon \quad (47)$$

$$\|z(t, \varepsilon) - h(t, \bar{x}(t)) - \hat{y}(t/\varepsilon)\| \leq k_2 \varepsilon \quad (48)$$

where  $\bar{x}(t)$  and  $\hat{y}(\tau)$  are the solutions of the reduced model (43) and boundary-layer model (44), respectively. Moreover, for any given  $T > t_0$ , there exists a positive constant  $\varepsilon^{**} \leq \varepsilon^*$  such that for  $t \in [T, \infty)$  and  $\varepsilon < \varepsilon^{**}$ , it follows uniformly that

$$\|z(t, \varepsilon) - h(t, \bar{x}(t))\| \leq k_3 \varepsilon \quad (49)$$

It means if  $\varepsilon$  is small enough, we can use the quasi-steady state  $h$  (solved from algebraic equations) + solution of boundary-layer model  $\hat{y}$  (solved from dynamic equations) to estimate the fast state; if  $\varepsilon$  is much smaller, then we can use only the quasi-steady state solution to estimate the fast state. This significantly reduce the computational complexity.

# Singular perturbation theory

The main difficulties focused on threefold:

- How to identify the slow and fast dynamics? (how to find the perturbation coefficients  $\varepsilon$ ?)
  - In most cases, we can find the small perturbation coefficients  $\varepsilon$  based on our knowledge of physical processes and components.
  - For linear systems, we can use modal analysis to identify the slow and fast dynamics. We can also obtain a local result for a linearized system.
- How to solve the quasi-steady state equation (41)?
  - We can apply implicit function theorem to check whether the solution of algebraic equation (41) can be expressed in closed form.
- How to obtain at least one isolated roots?
  - If the solutions are not isolated, sometimes we can get the isolated roots via coordinate transformation and redefining state variables.



# Order Reduction for WECC Composite Load Model

Consider the generic nonlinear state space model of WECC model

$$\dot{x}_{motori} = f(x_{motori}, u_{motor}, t) \quad (44)$$

$$y_{motor} = h(x_{motori}, u_{motor}, t) \quad (45)$$

$$\dot{x}_{DERA} = f(x_{DERA}, u_{DERA}, t) \quad (46)$$

$$y_{DERA} = h(x_{DERA}, u_{DERA}, t) \quad (47)$$

$$x_{motori} = [E'_{di}, E'_{qi}, E''_{di}, E''_{qi}, SLIP_i]^T \quad i = 1, 2, 3$$

$$u_{motor} = [V_{di} \ V_{qi}]^T \quad i = 1, 2, 3$$

$$y_{motori} = [P_i \ Q_i]^T \quad i = 1, 2, 3$$

$$x_{DERA} = [S_0, S_1, S_2, S_3, S_4, S_5, S_6, S_7, S_8, S_9]^T$$

$$u_{DERA} = [V_t \ Freq]^T$$

$$y_{DERA} = [P \ Q]^T$$

where the states, inputs and outputs are as follows

# Order reduction of DER\_A

Note that there are saturation, dead-zone and switch functions in the DER\_A model, therefore we cannot identify the slow and fast states via participation factor analysis. However, we can estimate the slow/fast classification by finding the perturbation coefficient.

Recall the dynamic equations of DER\_A, we can find the primary coefficients that affect the transient speed directly:  $T_V, T_P, T_{iq}, T_g, T_{rv}, T_{rf}, T_{pord}$ . If  $T_P, T_{rv}, T_{rf} \gg T_{iq}, T_g, T_V, T_{pord}$ , under the parameter setting in Table 2, using the order reduction technique introduced above, we can obtain the following **reduced order model of DER\_A**.

State equations:

$$\dot{x}_1 = \frac{1}{T_{rv}} (V_t - x_1) \quad (50)$$

$$\dot{x}_2 = \frac{1}{T_p} (x_4 - x_2) \quad (51)$$

$$\dot{x}_3 = \frac{1}{T_{rf}} (Freq - x_3) \quad (52)$$

$$\dot{x}_4 = 0 \quad (53)$$

Algebraic equations:

$$i_d = sat_9 \left( \frac{sat_7(x_4)}{sat_1(x_1)} \right) \times VoltageProtection(x_1, V_{rfrac}) + \hat{y}_{D2} \quad (54)$$

$$i_q = VoltageProtection(x_1, V_{rfrac}) \times sat_2 \left\{ \frac{Q_{gen0}}{P_{gen0}} \cdot \frac{x_2}{sat_1(x_1)} + K_{qv} \cdot sat_3 [DB_V (V_{ref0} - x_1)] \right\} + \hat{y}_{D6} \quad (55)$$

where  $x = [S_0, S_1, S_5, S_7] ([V_{tfilter}, P_{genfilter}, Freq_{filter}, U])$

Reduced system  
order from 10 to 4

# Order reduction of DER\_A

Boundary-layer model:

$$\dot{y}_{D1} = -y_{D1} \quad (56)$$

$$\dot{y}_{D2} = y_{D3} - y_{D2} - VoltageProtection(x_{D1}, V_{rfrac}) \times \{sat_2[\gamma(x_D)] + sat_2[y_{D1} + \gamma(x_D)]\} \quad (57)$$

$$\dot{y}_{D3} = -y_{D3} \quad (58)$$

$$\dot{y}_{D4} = -T_{rf} y_{D5} \quad (59)$$

$$\dot{y}_{D5} = -y_{D5} \quad (60)$$

$$\begin{aligned} \dot{y}_{D6} = & -y_{D6} - sat_9 \left[ \frac{sat_7(x_{D4})}{sat_1(x_{D1})} \right] \times VoltageProtection(x_{D1}, V_{rfrac}) \\ & + sat_9 \left[ \frac{sat_7(y_{D5} x_{D4})}{sat_1(x_{D1})} \right] \times [y_{D3} + VoltageProtection(x_{D1}, V_{rfrac})] \end{aligned} \quad (61)$$

$$\gamma(x_D) = \frac{\tan(pfaref)x_{D2}}{sat_1(x_{D1})} + K_{qv} sat_3[DB_V(V_{ref0} - x_{D1})] \quad (62)$$

# Order reduction of DER\_A

## Original

$$\dot{S}_0 = \frac{1}{T_{rv}} (V_t - S_0)$$

$$\dot{S}_1 = \frac{1}{T_p} (S_8 - S_1)$$

$$\dot{S}_2 = \begin{cases} -\frac{S_2}{T_{iq}} + \frac{Q_{ref}}{T_{iq} \text{sat}_1(S_0)} & \text{if } P_{fFlag} = 0 \\ -\frac{S_2}{T_{iq}} + \frac{\tan(\text{pf}_{aref}) \times S_1}{T_{iq} \text{sat}_1(S_0)} & \text{if } P_{fFlag} = 1 \end{cases}$$

$$\dot{S}_3 = \begin{cases} -\frac{S_3 - \text{sat}_2(S_2 + \text{sat}_3(DB_V(V_{ref0} - S_0) \cdot K_{qv}))}{T_g} & \text{if } V_{tripFlag} = 0 \\ -\frac{S_3 - \text{sat}_2(S_2 + \text{sat}_3(DB_V(V_{ref0} - S_0) \cdot K_{qv})) \times S_4}{T_g} & \text{if } V_{tripFlag} = 1 \end{cases}$$

$$\dot{S}_4 = \frac{1}{T_v} (\text{VoltageProtection}(S_0, V_{rfrac}) - S_4)$$

$$\dot{S}_5 = \frac{1}{T_{rf}} (Freq - S_5)$$

$$\dot{S}_6 = K_{ig} \text{sat}_4(P_{ref} - S_1 + \text{sat}_5[DB_F(Freq_{ref} - S_5)]) + \text{sat}_6[D_{up} \cdot DB_F(Freq_{ref} - S_5)] + \frac{K_{pg}}{T_p} S_1 + G_{dn}(Freq - S_5) + G_{up}(Freq - S_5) - \frac{K_{pg} S_8}{T_p}$$

$$\dot{S}_7 = \begin{cases} 0 & \text{if } Freq_{flag} = 0 \\ \text{sat}_8(\text{sat}_7(S_6)) & \text{if } Freq_{flag} = 1 \end{cases}$$

$$\dot{S}_8 = \frac{1}{T_{pord}} (S_7 - S_8)$$

$$\dot{S}_9 = \begin{cases} \frac{1}{T_g} \left( \text{sat}_9 \left( \frac{\text{sat}_7(S_8)}{\text{sat}_1(S_0)} \right) \times S_4 - S_9 \right) & \text{if } V_{tripFlag} = 1 \\ \frac{1}{T_g} \left( \text{sat}_9 \left( \frac{\text{sat}_7(S_8)}{\text{sat}_1(S_0)} \right) - S_9 \right) & \text{if } V_{tripFlag} = 0 \end{cases}$$

## Reduced

$$\dot{x}_1 = \frac{1}{T_{rv}} (V_t - x_1)$$

$$\dot{x}_2 = \frac{1}{T_p} (x_4 - x_2)$$

$$\dot{x}_3 = \frac{1}{T_{rf}} (Freq - x_3)$$

$$\dot{x}_4 = 0$$

$$i_d = \text{sat}_9 \left( \frac{\text{sat}_7(x_4)}{\text{sat}_1(x_1)} \right) \times \text{VoltageProtection}(x_1, V_{rfrac}) + \hat{y}_{D2} \quad (52)$$

$$i_q = \text{VoltageProtection}(x_1, V_{rfrac}) \times \text{sat}_2 \left\{ \frac{Q_{geno}}{P_{geno}} \cdot \frac{x_2}{\text{sat}_1(x_1)} + K_{qv} \cdot \text{sat}_3[DB_V(V_{ref0} - x_1)] \right\} + \hat{y}_{D6} \quad (53)$$

where  $x = [S_0, S_1, S_5, S_7] ([V_{filt}, P_{genfilt}, Freq_{filt}, U])$

- Simpler model structure and parameter set
- Still capture dynamic responses

# Simulation Results (DER\_A)

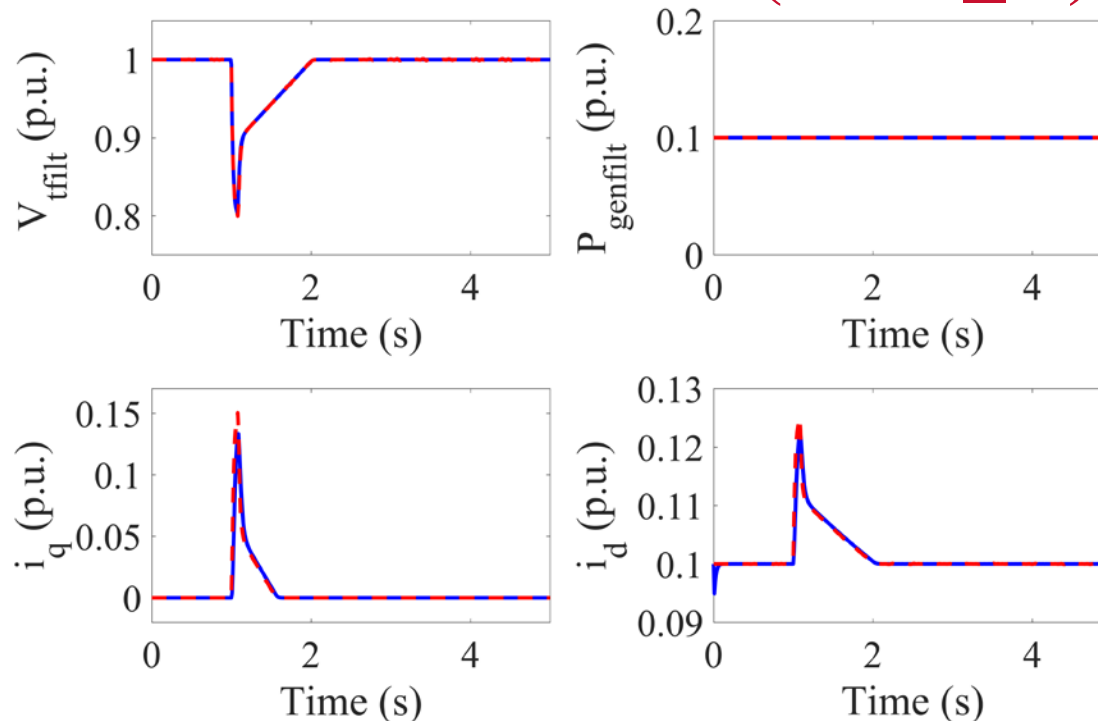


Fig. 12 Simulation results of reduced DER\_A model compared to original model. The figures show the results of  $V_{tfilt}$ ,  $P_{genfilt}$ ,  $i_d$ , and  $i_q$ . The red dashed line denotes the responses of reduced model, the blue solid line denotes that of original model.

# Simulation Results (DER\_A)

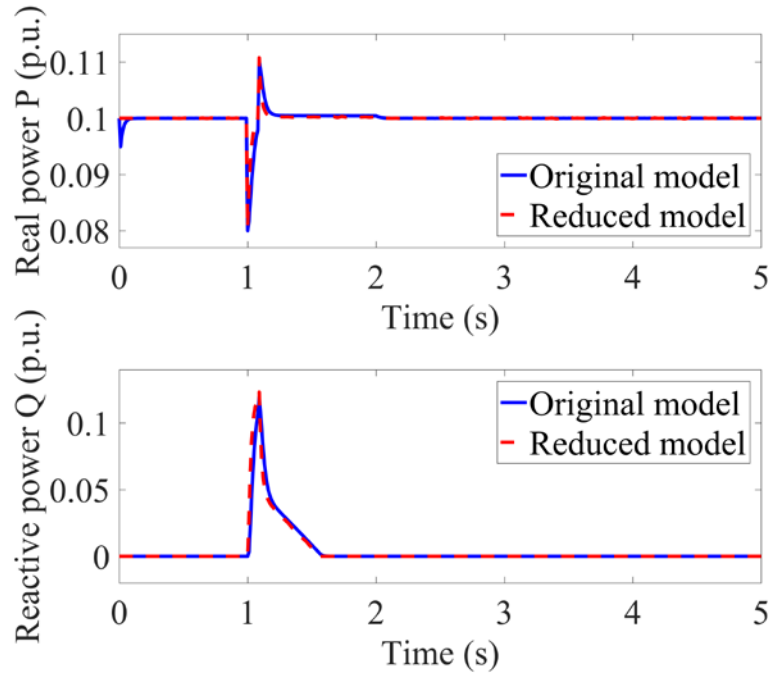


Fig. 13 The figures show the results of real and reactive power. The red dashed line denotes the responses of reduced model, the blue solid line denotes that of original model.

The computation time of original model and reduced model are 4.8025 s and 1.1623 s, respectively.

Note that the reduced model depends on the parameters of switching functions, because they change the model structure.

For example, if  $Freq_{flag}$  in equation (33) is set to be 1

$$\dot{S}_7 = \begin{cases} 0 & \text{if } Freq_{flag} = 0 \\ sat_8(sat_7(S_6)) & \text{if } Freq_{flag} = 1 \end{cases} \quad (33)$$

then  $S_7$  will be identified as fast state, thus the load model will be further reduced to 3 instead of 4.

# Participation factor analysis (three-phase motor)

Use numerical methods to solve the load model, obtaining one equilibrium.



Calculate the eigenvalues at the equilibrium and determine the modes.



Calculate the participation factors using the following formula:

$$P_{ij} = \frac{|u_{ij}^T| |v_{ij}|}{\sum_{k=1}^N |u_{kj}^T| |v_{jk}|}$$



Identify the slow/fast dynamics according to the participation factors and corresponding eigenvalues.

# Participation factor analysis (three phase motor)

Index	Eigenvalues	Major participants
1, 2	$-11.04072 \pm 299207.1i$	$E'_{q1}, E'_{d1}$
6, 7	$-11.33576 \pm 299151.8i$	$E'_{q2}, E'_{d2}$
11, 12	$-11.33576 \pm 299151.8i$	$E'_{q3}, E'_{d3}$
5	-0.00096	$SLIP_1$
10	-0.00096	$SLIP_2$
15	-0.00096	$SLIP_3$
3, 4	$-499.829 \pm 299120.1i$	$E''_{q1}, E''_{d1}$
8, 9	$-383.280 \pm 299134.5i$	$E''_{q2}, E''_{d2}$
13, 14	$-383.280 \pm 299134.5i$	$E''_{q3}, E''_{d3}$

Slow

Fast



# Order reduction of three-phase motor

Note that the above modal decomposition results is consistent with the comparison between  $T_{po}$  and  $T_{ppo}$ . According to the above slow and fast identification, using the singular perturbation theory, defining  $x = [E'_q, E'_d, SLIP]$ ,  $U = [V_q, V_d]$ , we can obtain the reduced order large signal model of three-phase motor as follows,

State equations: 
$$\dot{x}_1 = \frac{1}{T_{p0}} [-x_1 - i_d(L_s - L_p) - \omega_0 T_{p0} x_2 x_3] \quad (63)$$

$$\dot{x}_2 = \frac{1}{T_{p0}} [-x_2 + i_q(L_s - L_p) + \omega_0 T_{p0} x_1 x_3] \quad (64)$$

$$\dot{x}_3 = -\frac{p \cdot h_2(x_1, x_2, x_3) \cdot i_d + q \cdot h_1(x_1, x_2, x_3) \cdot i_q - TL}{2H} \quad (65)$$

Reduced system  
order from 5 to 3

Algebraic equations: 
$$h_1(x_1, x_2, x_3) = \frac{1}{r_s^2 + L_p^2} [(L_p L_{pp} + r_s^2)x_1 - (L_p - L_{pp})r_s x_2 - (L_p - L_{pp})L_p U_1 - (L_p - L_{pp})r_s U_2] \quad (66)$$

$$h_2(x_1, x_2, x_3) = \frac{1}{r_s^2 + L_p^2} [(L_p - L_{pp})r_s x_1 - (L_p L_{pp} + r_s^2)x_2 + (L_p - L_{pp})r_s U_1 - (L_p - L_{pp})L_p U_2] \quad (67)$$

$$i_q = \frac{r_s}{r_s^2 + L_p^2} (U_1 + x_1) - \frac{L_p}{r_s^2 + L_p^2} (U_2 + x_2) \quad (68)$$

$$i_d = \frac{L_p}{r_s^2 + L_p^2} (U_1 + x_1) + \frac{r_s}{r_s^2 + L_p^2} (U_2 + x_2) \quad (69)$$

$$TL = (p \cdot h_2(x_1, x_2, x_3) \cdot i_d + q \cdot h_1(x_1, x_2, x_3) \cdot i_q)(A(1 - x_3)^2 + B(1 - x_3) + C_0 + D(1 - x_3)^{Etrq}) \quad (70)$$

Quasi-steady  
state solution

# Simulation Results (Motor A)

The computation time of original model and reduced model are 2.8176 s and 0.9023 s, respectively.

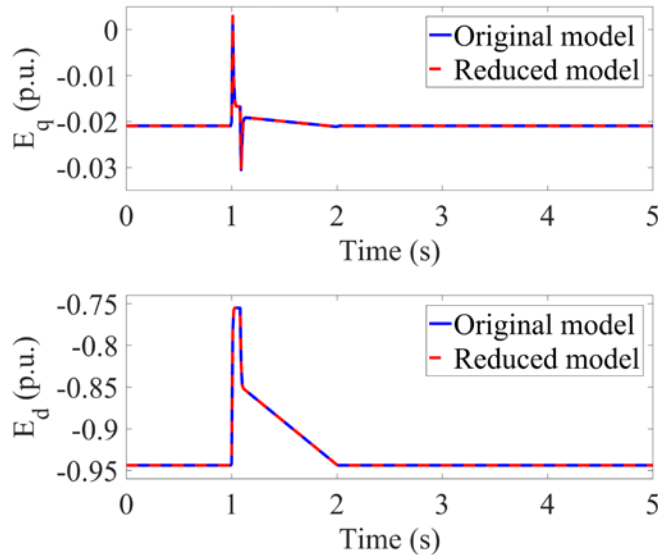


Fig. 14 Simulation results  $E'_d$  and  $E'_q$  of reduced three-phase motor A compared to original model.

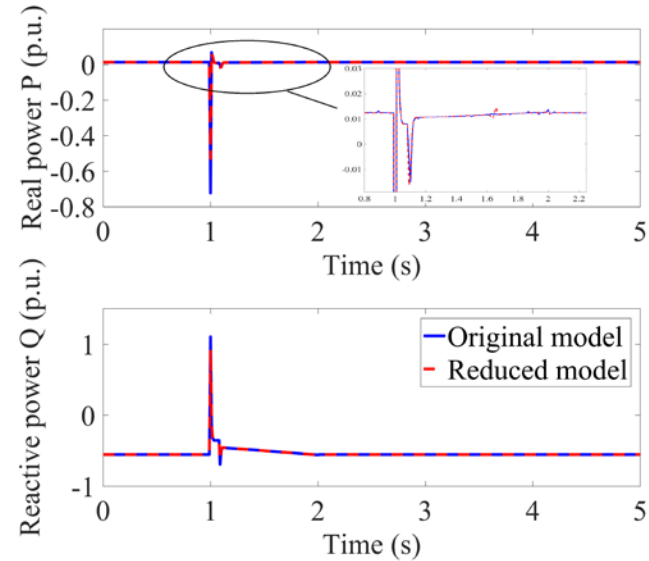


Fig. 15 Simulation results of real and reactive power of reduced three-phase motor A compared to original model.

# Simulation Results (Motor B)

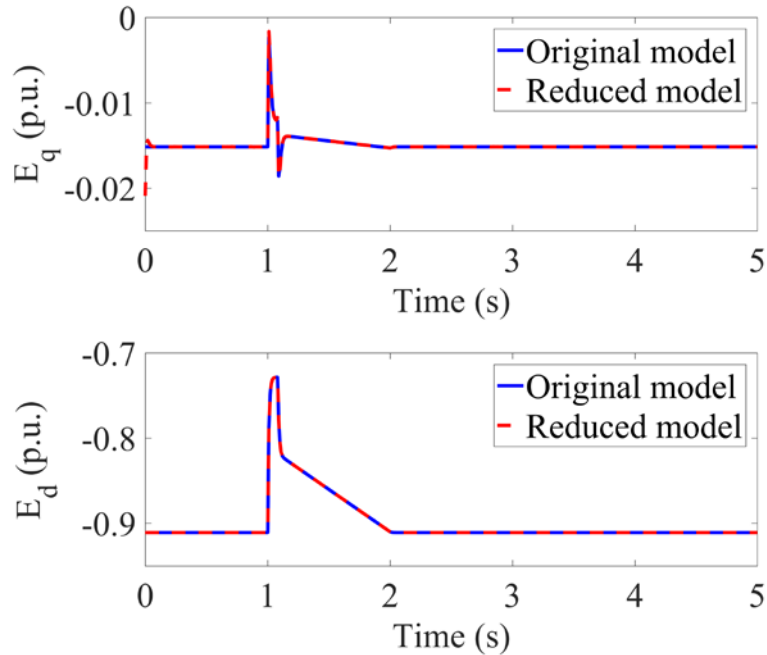


Fig. 16 Simulation results  $E'_d$  and  $E'_q$  of reduced three-phase motor B compared to original model.

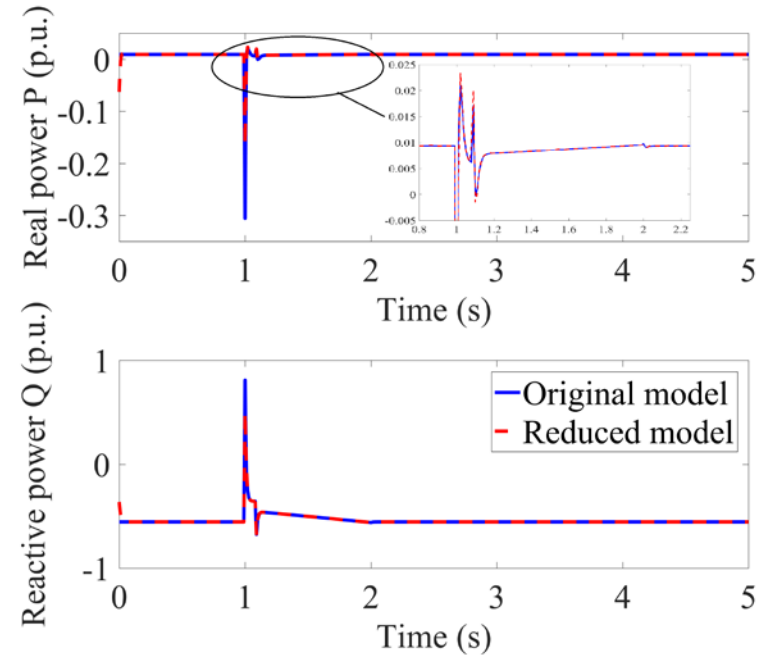


Fig. 17 Simulation results of real and reactive power of reduced three-phase motor B compared to original model.

# Simulation Results (Motor C)

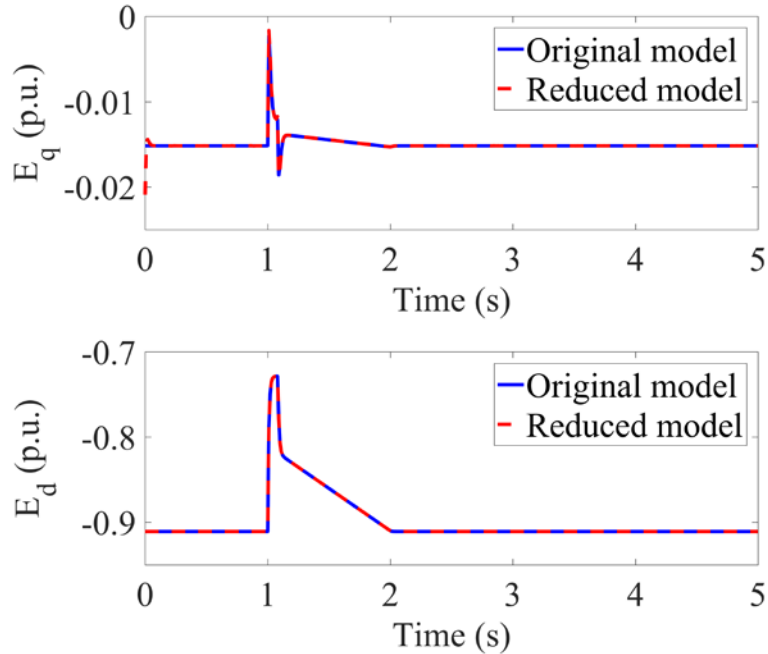


Fig. 16 Simulation results  $E'_d$  and  $E'_q$  of reduced three-phase motor C compared to original model.

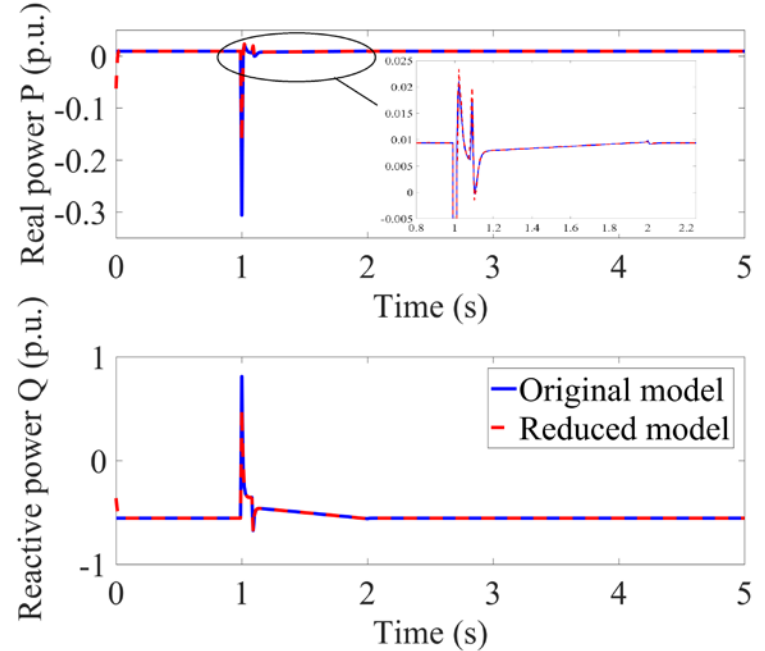


Fig. 17 Simulation results of real and reactive power of reduced three-phase motor C compared to original model.

- Mathematical representation of WECC composite load model
- Dynamic order reduction of WECC composite load model
- **Robust Time Varying Parameter Identification for Composite Loads**
- SVM-Based Parameter Identification for Composite ZIP and Electronic Load Modeling

# Background and motivation

- With the increasing integration of uncertain resources, e.g., renewable energy, electric vehicles, and demand response, it is imperative to design robust load modeling methods.
- The integration of uncertain resources results in continuous changes of load model parameters, thus requiring time-varying parameter identification.
- The composite models, including ZIP models and induction motor (IM) models, are most widely used for dynamic analysis in the US industry.

## Equivalent circuit of ZIP + IM model

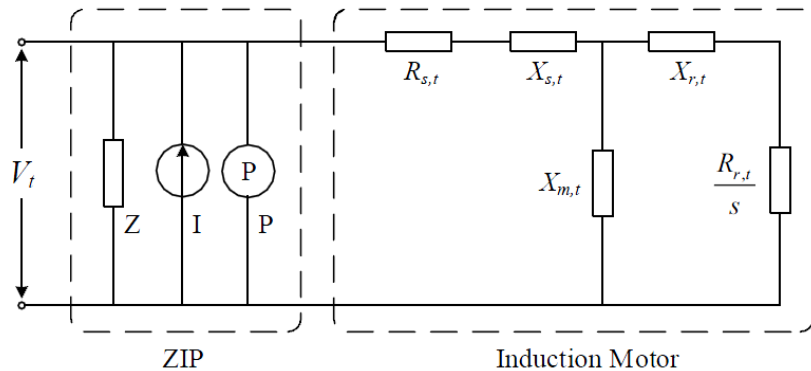


Fig. 18 Equivalent circuit of ZIP and IM load model.

## ZIP Model

$$P_{ZIP,t} = P_{ZIP,0} \left( a_{p,t} \left( \frac{V_t}{V_0} \right)^2 + b_{p,t} \left( \frac{V_t}{V_0} \right) + c_{p,t} \right) \quad (71)$$

$$Q_{ZIP,t} = Q_{ZIP,0} \left( a_{q,t} \left( \frac{V_t}{V_0} \right)^2 + b_{q,t} \left( \frac{V_t}{V_0} \right) + c_{q,t} \right) \quad (72)$$

## IM Model

$$\frac{dv'_{d,t}}{dt} = \frac{-R_{r,t}}{X_{r,t} + X_{m,t}} \left( v'_{d,t} + \frac{X_{m,t}^2}{X_{r,t} + X_{m,t}} i_{q,t} \right) + s_t v'_{q,t} \quad (73)$$

$$\frac{dv'_{q,t}}{dt} = \frac{-R_{r,t}}{X_{r,t} + X_{m,t}} \left( v'_{q,t} - \frac{X_{m,t}^2}{X_{r,t} + X_{m,t}} i_{d,t} \right) - s_t v'_{d,t} \quad (74)$$

$$\frac{ds_t}{dt} = \frac{1}{2H_t} \left( T_{m0}(1 - s_t)^2 - v'_{d,t} i_{d,t} - v'_{q,t} i_{q,t} \right) \quad (75)$$

$$i_{d,t} = \frac{R_{s,t}(U_{d,t} - v'_{d,t}) + X'_t(U_{q,t} - v'_{q,t})}{R_{s,t}^2 + X_t'^2} \quad (76)$$

$$i_{q,t} = \frac{R_{s,t}(U_{q,t} - v'_{q,t}) - X'_t(U_{d,t} - v'_{d,t})}{R_{s,t}^2 + X_t'^2} \quad (77)$$

$$V_t = \sqrt{U_{d,t}^2 + U_{q,t}^2} \quad (78) \quad X'_t = X_{s,t} + \frac{X_{m,t} \cdot X_{r,t}}{X_{m,t} + X_{r,t}} \quad (79)$$

$$P_{IM,t} = \left[ R_{s,t}(U_{d,t}^2 + U_{q,t}^2 - U_{d,t}v'_{d,t} - U_{q,t}v'_{q,t}) - X'_t(U_{d,t}v'_{q,t} - U_{q,t}v'_{d,t}) \right] / (R_{s,t}^2 + X_t'^2) \quad (80)$$

$$Q_{IM,t} = \left[ X'_t(U_{d,t}^2 + U_{q,t}^2 - U_{d,t}v'_{d,t} - U_{q,t}v'_{q,t}) - R_{s,t}(U_{d,t}v'_{q,t} - U_{q,t}v'_{d,t}) \right] / (R_{s,t}^2 + X_t'^2) \quad (81)$$

# Proposed framework of robust time-varying parameter identification

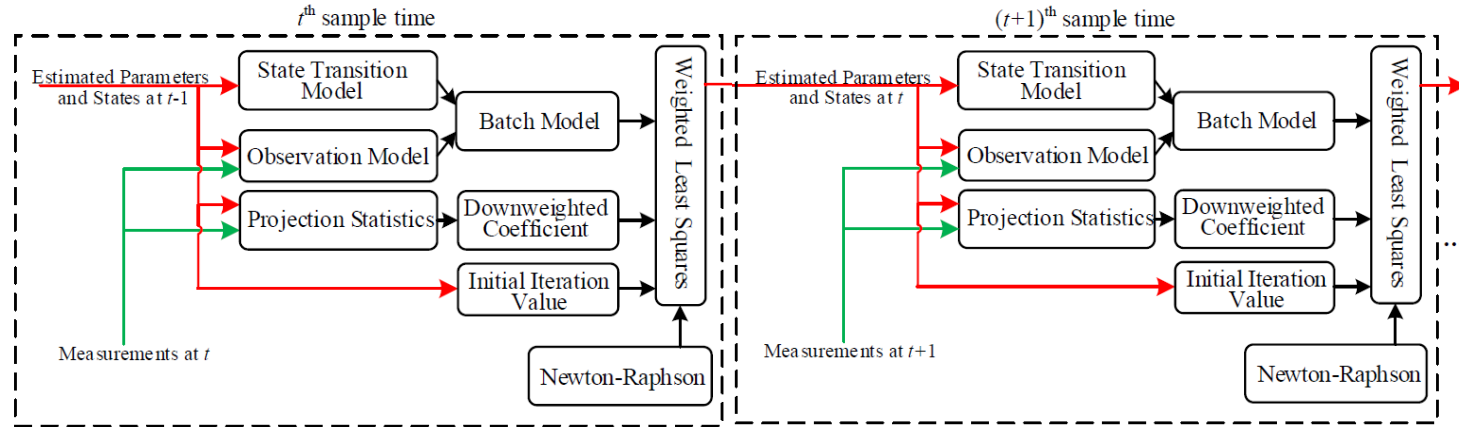


Fig. 19 Framework of robust time-varying parameter identification.



# Simulation Results

## Case 1 (IEEE 57-bus system)

- The IEEE 57-bus system in which 20 buses are connected to composite ZIP and IM loads are used to validate the proposed method.
- For each composite ZIP and IM load, there are 500 samples for simulation, and the sample time is 0.1s.
- To illustrate the results, we only focus on the measurements of the bus of interest, i.e., bus No. 11.

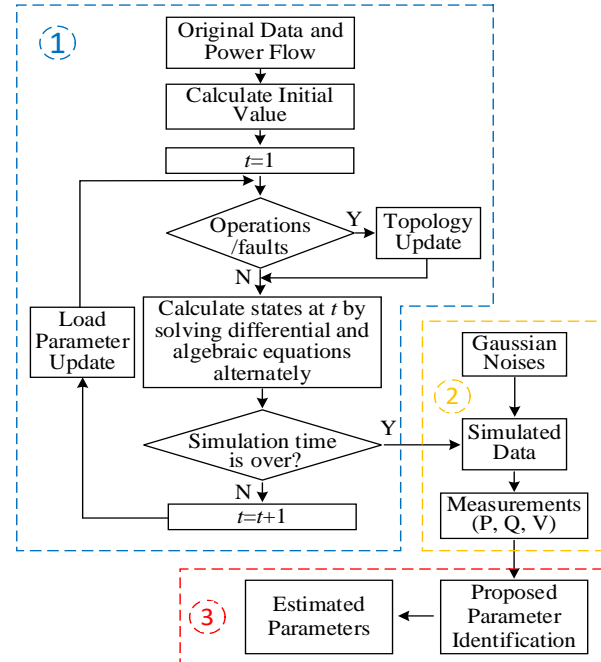


Fig. 20 Simulation processes.

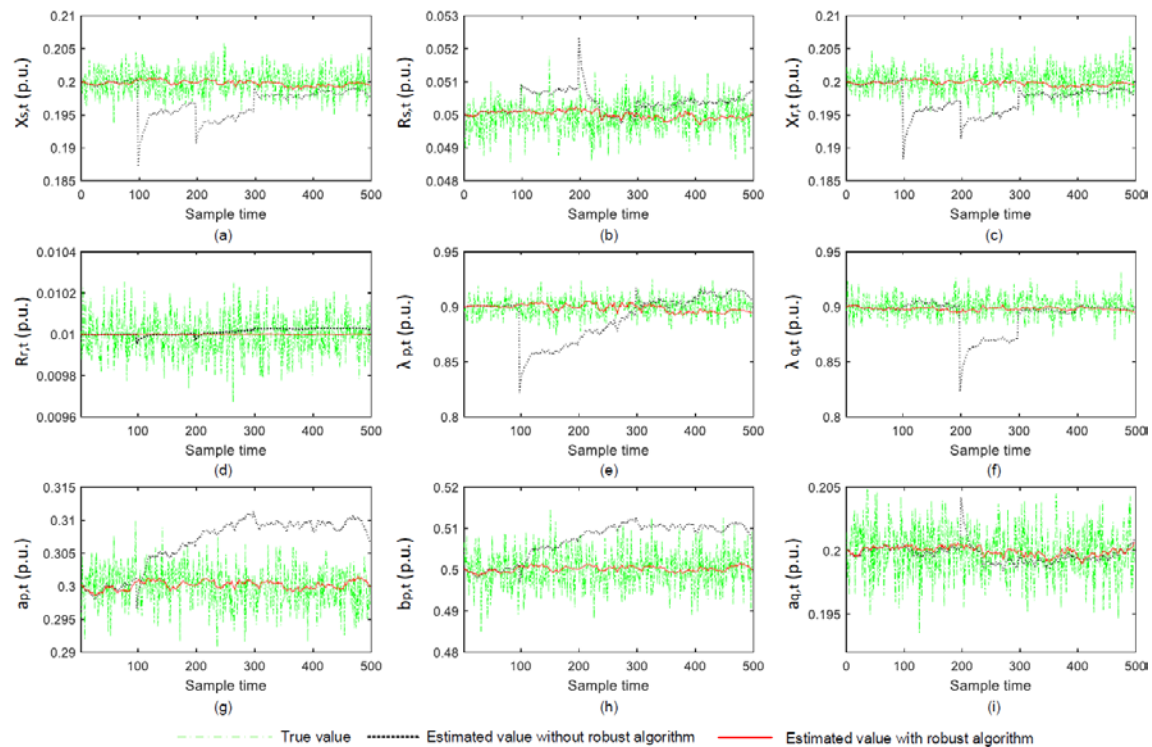


Fig. 21 Parameter identification results comparison for (a)  $X_s$ , (b)  $R_s$ , (c)  $X_r$ , (d)  $R_r$ , (e)  $\lambda_p$ , (f)  $\lambda_q$ , (g)  $a_p$ , (h)  $b_p$ , (i)  $a_q$ .

At sample 100, real power measurement has a outlier; At sample 200, reactive power measurement has a outlier; At samples 300 and 400, voltage measurements have outliers.

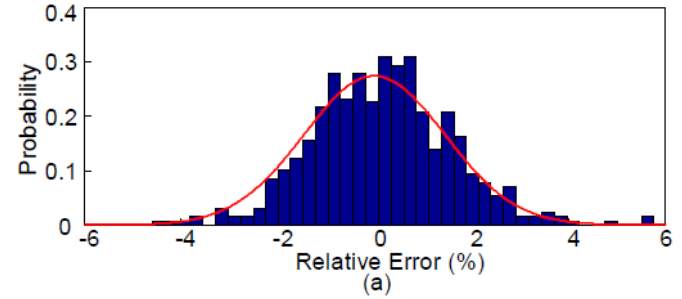
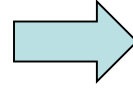
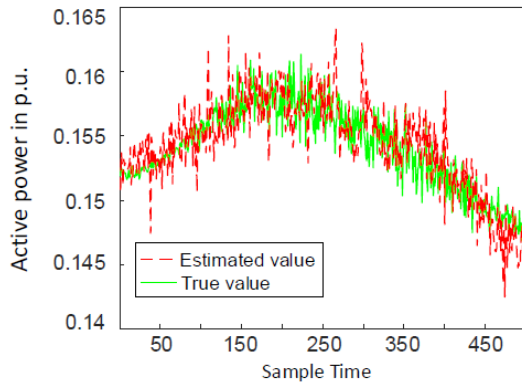


Fig. 22 Estimated active power and true active power.

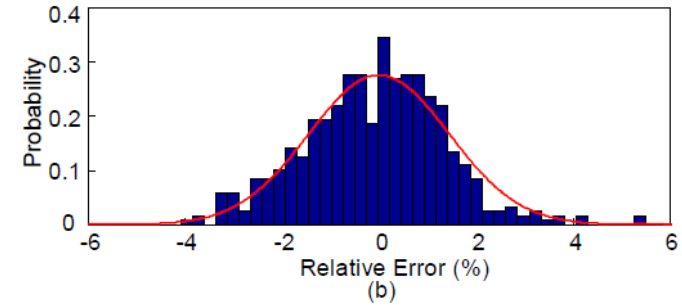
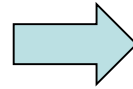
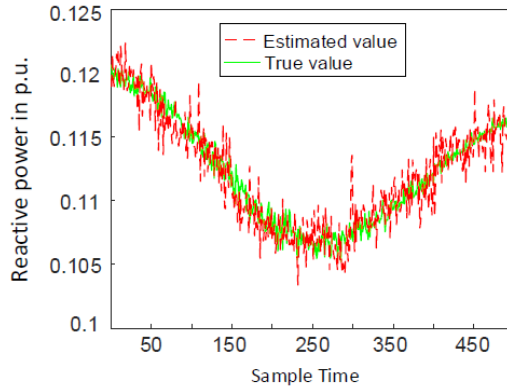


Fig. 23 Estimated reactive power and true reactive power.

Fig. 24 (a) Relative errors of estimated active power. (b) Relative errors of estimated reactive power.

## Case 2 (IEEE 118-bus system)

- The IEEE 118-bus system in which 50 buses are connected to composite ZIP and IM loads are used to validate the proposed method. Table XV shows the buses with composite ZIP and IM loads.
- For each composite ZIP and IM load, there are 500 samples for simulation, and the sample time is 0.1s.
- To illustrate the results, we only focus on the measurements of the bus of interest, i.e., bus No. 11.

Table III  
Buses with ZIP and IM loads

Buses with composite ZIP and IM loads
2, 3, 5, 7, 9, 11, 13, 16, 17, 20, 21, 22, 23, 28, 29
30, 33, 35, 37, 38, 39, 41, 43, 44, 45, 47, 48, 50, 51, 52
53, 57, 58, 60, 63, 64, 67, 68, 71, 75, 78, 79, 81, 82, 83
84, 86, 88, 93, 94

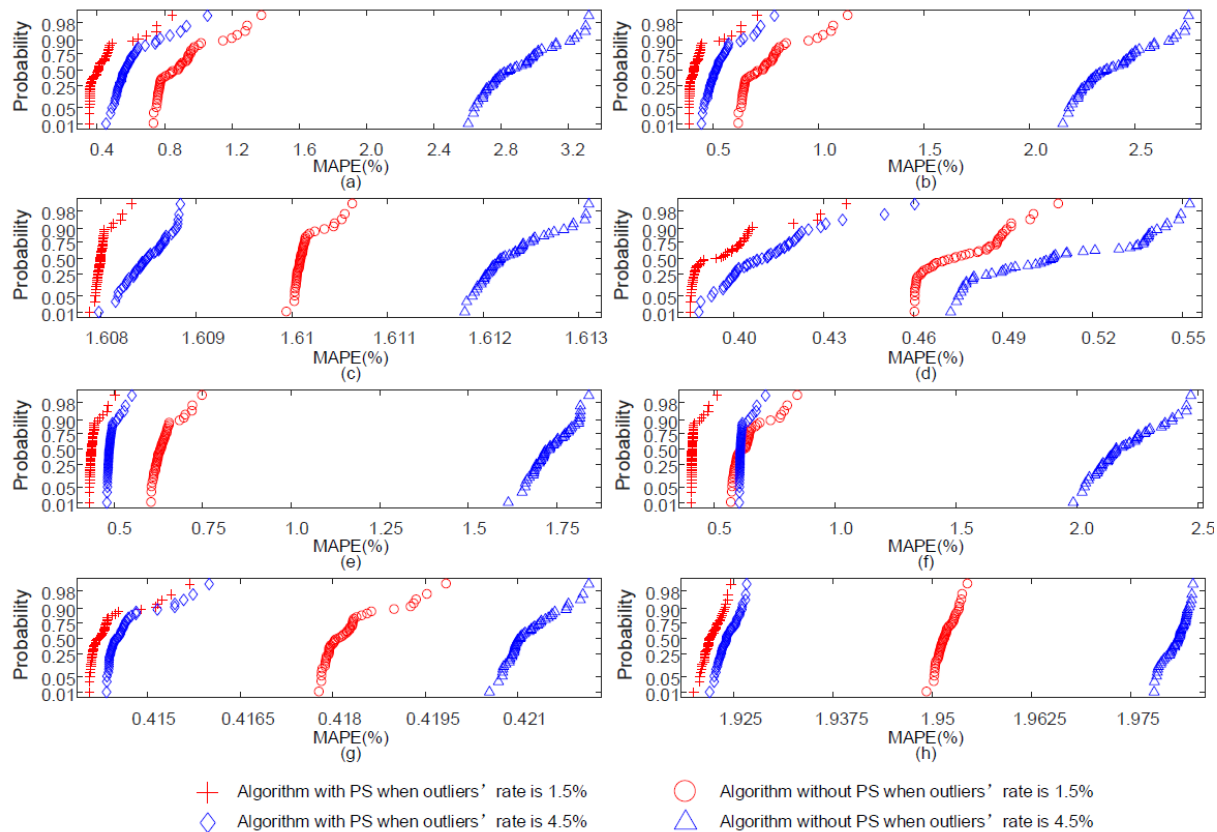


Fig. 25 Mean absolute percentage errors (MAPEs) of for (a)  $X_s$ , (b)  $R_s$ , (c)  $X_r$ , (d)  $R_r$ , (e)  $\lambda_p$ , (f)  $\lambda_q$ , (g)  $a_p$ , (h)  $b_p$ , (i)  $a_q$ .

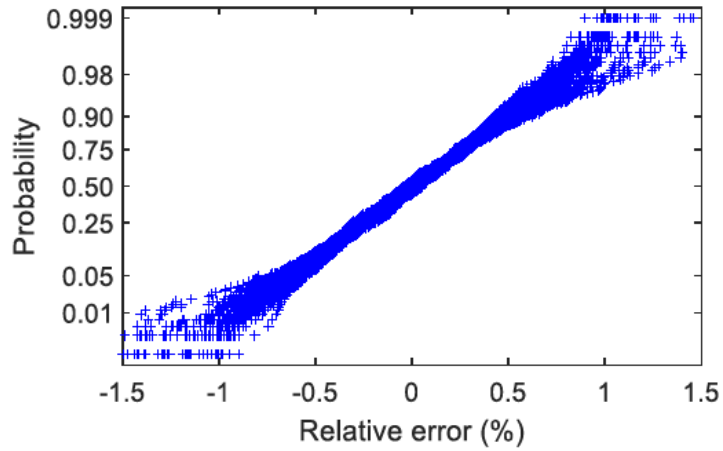


Fig. 26 Probability of relative errors of estimated active power of the composite ZIP and IM loads at different buses in IEEE 118-bus system.

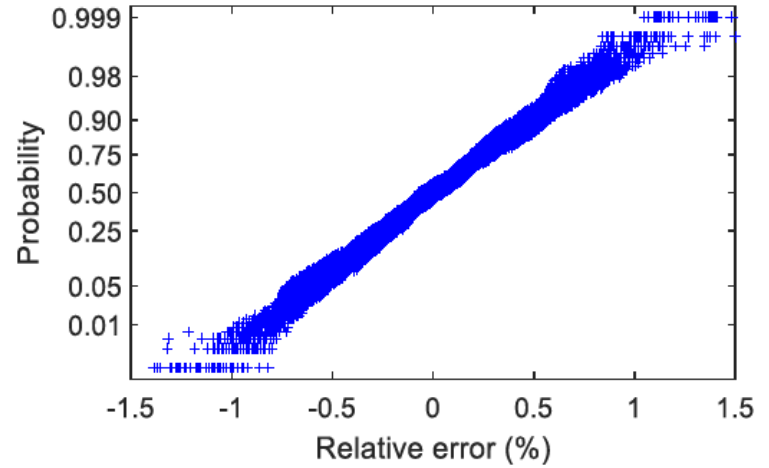


Fig. 27 Probability of relative errors of estimated reactive power of the composite ZIP and IM loads at different buses in IEEE 118-bus system.

- Mathematical representation of WECC composite load model
- Dynamic order reduction of WECC composite load model
- Robust Time Varying Parameter Identification for Composite Loads
- **SVM-Based Parameter Identification for Composite ZIP and Electronic Load Modeling**

# Background and motivation

- Electronic devices continue to grow and their operating characteristics are different from the conventional loads.
- We propose a composite ZIP and Electronic Load model.
- However, incorporating electronic loads will introduce high nonlinearity to models. Hence, we propose a data-driven and learning-based approach to identify model parameters.
- Specifically, we use a piecewise function to approximate electronic models and we design a Support Vector Machine (SVM)-based algorithm to identify model parameters.

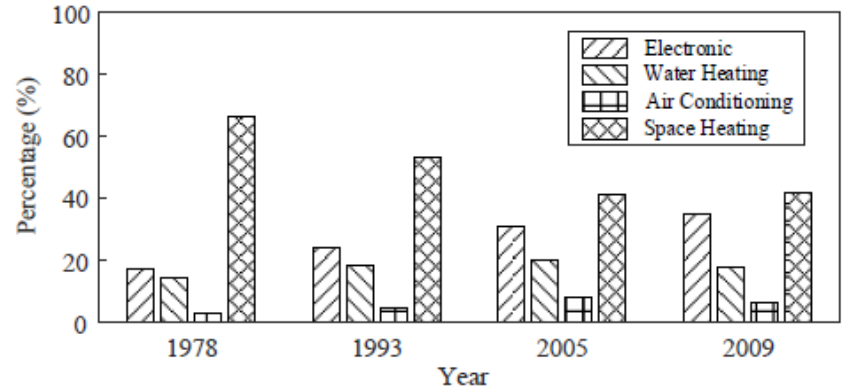


Fig. 28. Statistical data of typical energy consumption in homes by end uses in 1978 (a), 1993 (b), 2005 (c), and 2009 (d).



# Framework of Proposed Parameter Identification

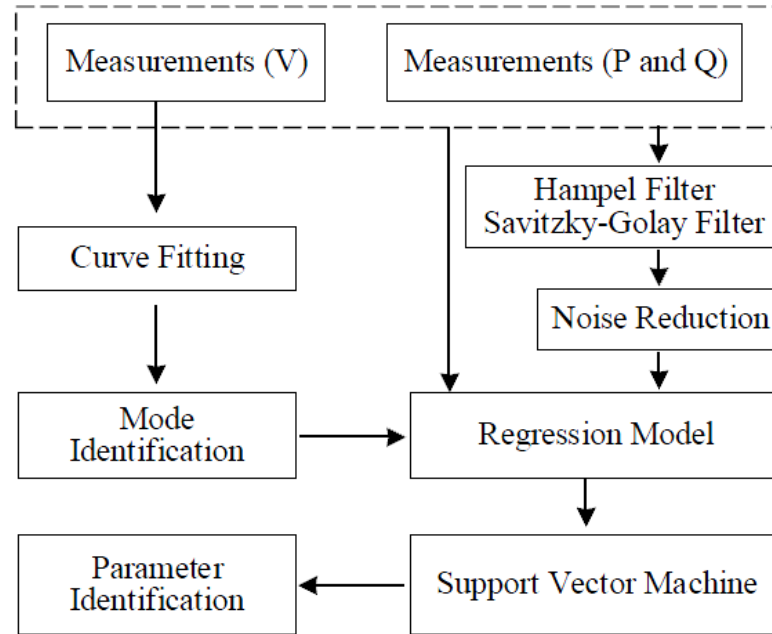


Fig. 29 Framework of the proposed method.

# ZIP and Electronic Models

## Electronic model

$$P_{E,t} = c_t \cdot P_{E,0} \quad (82)$$

$$Q_{E,t} = c_t \cdot Q_{E,0} \quad (83)$$

Table IV  
DIFFERENT MODES OF ELECTRONIC LOADS

Value of $c_t$	Condition	Mode
0	$V_t < V_{d2}$	1
$\frac{V_t - V_{d2}}{V_{d1} - V_{d2}}$	$V_{d2} \leq V_t < V_{d1}, V_t \leq V_{\min,t}$	2
$\frac{V_{\min,t} - V_{d2} + \alpha \cdot (V_t - V_{\min,t})}{V_{d1} - V_{d2}}$	$V_{d2} \leq V_t < V_{d1}, V_t > V_{\min,t}$	3
1	$V_t \geq V_{d1}, V_{\min,t} \geq V_{d1}$	4
$\frac{V_{\min,t} - V_{d2} + \alpha \cdot (V_{d1} - V_{\min,t})}{V_{d1} - V_{d2}}$	$V_t \geq V_{d1}, V_{\min,t} < V_{d1}$	5

In Table IV,  $V_{d1}$  and  $V_{d2}$  are two threshold values, and  $\alpha$  is a fraction of the electronic load that recovers from low voltage trip.  $V_{\min,t}$  is a value tracking the lowest voltage but not below  $V_{d2}$ , and it is a known value at each sample. Its value can be expressed as follows.

$$V_{\min,t} = \max \{V_{d2}, \min \{V_t, V_{\min,t-1}\}\} \quad (84)$$

# ZIP and Electronic Models

## Composite ZIP & Electronic model

$$P_t = \lambda_1 \cdot V_t^2 + \lambda_2 \cdot V_t + \lambda_3 \quad (85)$$

Table V  
PARAMETERS FOR ACTIVE POWER OF COMPOSITE MODEL

Mode	$\lambda_1$	$\lambda_2$	$\lambda_3$
1	$(1 - \beta_p) \cdot \frac{P_{ZIP,0} \cdot a_p}{V_0^2}$	$(1 - \beta_p) \cdot \frac{P_{ZIP,0} \cdot b_p}{V_0}$	$(1 - \beta_p) \cdot P_{ZIP,0} \cdot c_p$
2	$(1 - \beta_p) \cdot \frac{P_{ZIP,0} \cdot a_p}{V_0^2}$	$(1 - \beta_p) \cdot \frac{P_{ZIP,0} \cdot b_p}{V_0} + \beta_p \cdot \frac{P_{E,0}}{V_{d1} - V_{d2}}$	$(1 - \beta_p) \cdot P_{ZIP,0} \cdot c_p - \beta_p \cdot \frac{P_{E,0} \cdot V_{d2}}{V_{d1} - V_{d2}}$
3	$(1 - \beta_p) \cdot \frac{P_{ZIP,0} \cdot a_p}{V_0^2}$	$(1 - \beta_p) \cdot \frac{P_{ZIP,0} \cdot b_p}{V_0} + \beta_p \cdot \frac{P_{E,0} \cdot \alpha}{V_{d1} - V_{d2}}$	$(1 - \beta_p) \cdot P_{ZIP,0} \cdot c_p + \beta_p \cdot \frac{P_{E,0} (V_{min,t} - V_{d2} - \alpha \cdot V_{min,t})}{V_{d1} - V_{d2}}$
4	$(1 - \beta_p) \cdot \frac{P_{ZIP,0} \cdot a_p}{V_0^2}$	$(1 - \beta_p) \cdot \frac{P_{ZIP,0} \cdot b_p}{V_0}$	$(1 - \beta_p) \cdot P_{ZIP,0} \cdot c_p + \beta_p \cdot P_{E,0}$
5	$(1 - \beta_p) \cdot \frac{P_{ZIP,0} \cdot a_p}{V_0^2}$	$(1 - \beta_p) \cdot \frac{P_{ZIP,0} \cdot b_p}{V_0}$	$(1 - \beta_p) \cdot P_{ZIP,0} \cdot c_p + \beta_p \cdot \frac{P_{E,0} (V_{min,t} - V_{d2} + \alpha \cdot V_{d1} - \alpha \cdot V_{min,t})}{V_{d1} - V_{d2}}$

# Simulation Results

Case 1: A revised IEEE 123-bus system is used for simulations. To illustrate the results, we focus on the measurements of bus 6 which is connected with a composite ZIP and electronic load.

Table VI  
PARAMETERS OF COMPOSITE LOAD

Parameters	Values (p.u.)	Parameters	Values (p.u.)
$P_{ZIP,0}$	0.80	$Q_{ZIP,0}$	0.40
$a_p$	0.20	$b_p$	0.40
$c_p$	0.40	$a_q$	0.15
$b_q$	0.35	$c_q$	0.50
$V_{d1}$	0.95	$V_{d2}$	0.70
$\alpha$	0.25	$P_{E,0}$	0.45
$Q_{E,0}$	0.30	$\beta$	0.40
$V_0$	1.00		

To test the model and the identification algorithm, one thousand operating points are simulated to obtain the true values including voltage and power. Then, noises are added to the true values to generate the signals. The noises are assumed to follow a Gaussian distribution. To compare the results, we consider one thousand scenarios, and each scenario has one thousand sample points with different noises added to the true values.

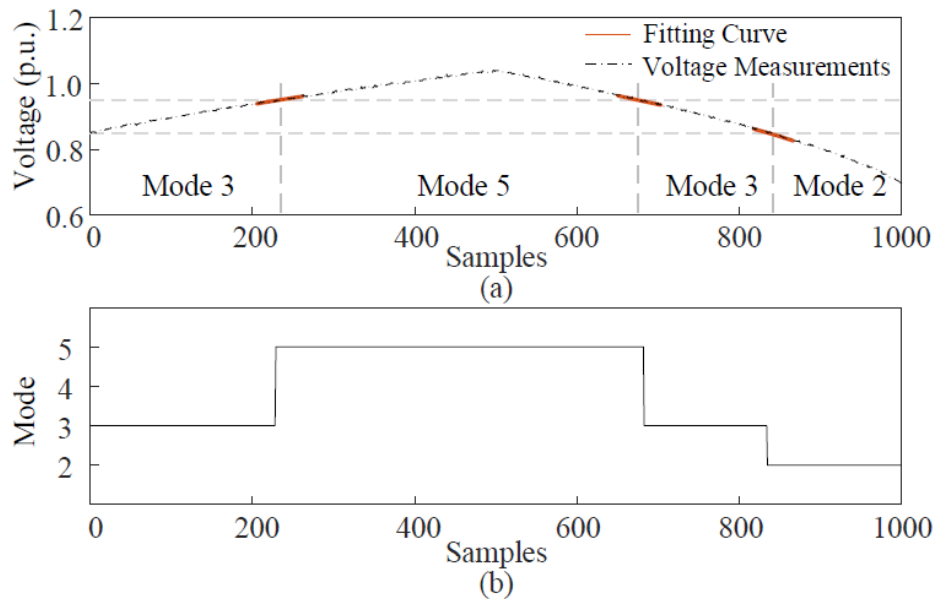


Fig. 29 (a) Voltage measurements and fitting curve. (b) Operating modes at different samples.

TABLE VII  
ESTIMATIONS OF  $\lambda_1$

	True Value	SVM	H-SVM	SG-SVM
Mode3	0.0960	0.1025	0.0995	0.0989
Mode5	0.0960	0.1004	0.0985	0.0981
Mode2	0.0960	0.1028	0.0990	0.0986

TABLE VIII  
ESTIMATIONS OF  $\lambda_2$

	True Value	SVM	H-SVM	SG-SVM
Mode3	0.3720	0.3602	0.3656	0.3666
Mode5	0.1920	0.1833	0.1871	0.1878
Mode2	0.9120	0.9012	0.9072	0.9078

TABLE IX  
ESTIMATIONS OF  $\lambda_3$

	True Value	SVM	H-SVM	SG-SVM
Mode3	0.1503	0.1556	0.1531	0.1527
Mode5	0.3213	0.3256	0.3237	0.3234
Mode2	-0.3120	-0.3077	-0.3101	-0.3103

Case 2: To further test the algorithm, additional voltage curves are used. The test system and the parameters are the same as the scenario in Case 1.

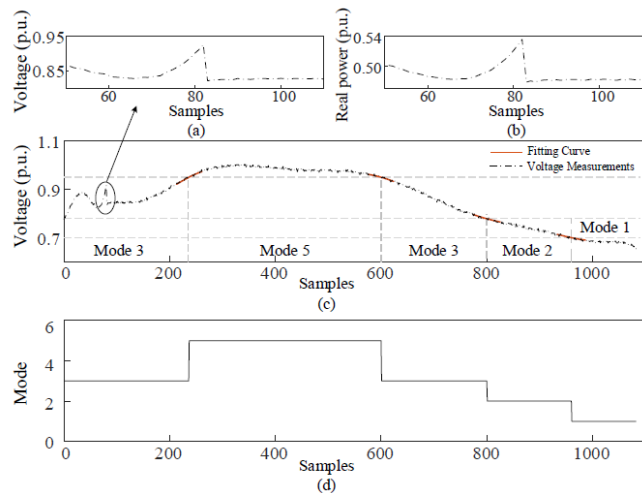


Fig. 30 (a) Voltage measurements and fitting curve. (b) Operating modes at different samples.

TABLE X  
RES OF ESTIMATED PARAMETERS WITH DIFFERENT APPROACHES  
UNDER THE MODE 3

		RE (%)		
		$\lambda_1$	$\lambda_2$	$\lambda_3$
Algorithm	SVM	3.8096	3.7222	1.2502
	H-SVM	1.4945	1.4567	0.4881
	SG-SVM	1.3425	1.3081	0.4382

TABLE XI  
RES OF ESTIMATED PARAMETERS WITH DIFFERENT APPROACHES  
UNDER THE MODE 5

		RE (%)		
		$\lambda_1$	$\lambda_2$	$\lambda_3$
Algorithm	SVM	3.2434	1.4514	2.1558
	H-SVM	2.2573	1.0089	1.4973
	SG-SVM	1.9042	0.8514	1.2642

TABLE XII  
RES OF ESTIMATED PARAMETERS WITH DIFFERENT APPROACHES  
UNDER THE MODE 2

		RE (%)		
		$\lambda_1$	$\lambda_2$	$\lambda_3$
Algorithm	SVM	3.7946	2.4658	2.1368
	H-SVM	2.6245	1.6136	1.3539
	SG-SVM	1.8349	1.1489	0.9387

TABLE XIII  
RES OF ESTIMATED PARAMETERS WITH DIFFERENT APPROACHES  
UNDER THE MODE 1

		RE (%)		
		$\lambda_1$	$\lambda_2$	$\lambda_3$
Algorithm	SVM	4.2486	4.3978	3.1454
	H-SVM	2.9223	2.1284	1.8354
	SG-SVM	1.5445	1.4543	1.1254

Case 3: To further test the algorithm, additional voltage curves are used. The test system and the parameters are the same as the scenario in Case 1.

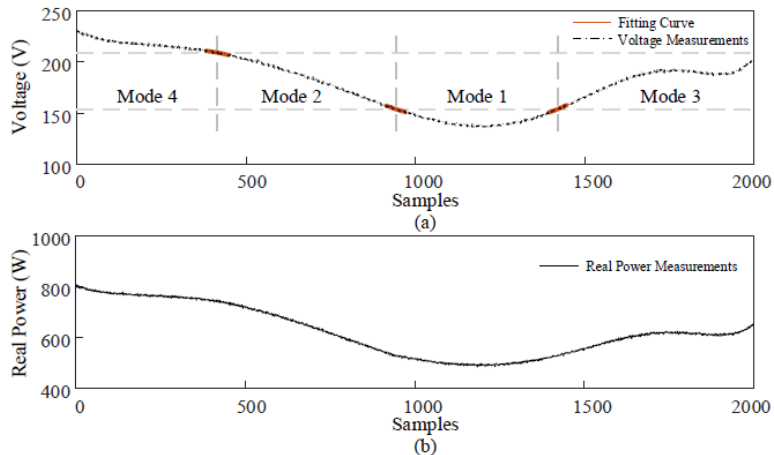


Fig. 31 (a) Voltage measurements and fitting curve. (b) Operating modes at different samples.

TABLE XIV  
RES OF ESTIMATED PARAMETERS WITH DIFFERENT APPROACHES UNDER THE MODE 4

		RE (%)		
		$\lambda_1$	$\lambda_2$	$\lambda_3$
Algorithm	SVM	5.1011	5.5973	2.3383
	H-SVM	3.6899	4.0456	1.6889
	SG-SVM	3.3067	3.6281	1.5158

TABLE XV  
RES OF ESTIMATED PARAMETERS WITH DIFFERENT APPROACHES UNDER THE MODE 2

		RE (%)		
		$\lambda_1$	$\lambda_2$	$\lambda_3$
Algorithm	SVM	2.8268	1.2071	9.3492
	H-SVM	2.6826	1.1472	8.8973
	SG-SVM	2.3242	0.9923	7.6816

TABLE XVI  
RES OF ESTIMATED PARAMETERS WITH DIFFERENT APPROACHES UNDER THE MODE 1

		RE (%)		
		$\lambda_1$	$\lambda_2$	$\lambda_3$
Algorithm	SVM	4.8501	3.5064	1.2659
	H-SVM	3.8437	2.7783	1.0029
	SG-SVM	3.4770	2.5142	0.9079

TABLE XVII  
RES OF ESTIMATED PARAMETERS WITH DIFFERENT APPROACHES UNDER THE MODE 3

		RE (%)		
		$\lambda_1$	$\lambda_2$	$\lambda_3$
Algorithm	SVM	3.2761	2.2586	1.6355
	H-SVM	3.1485	2.1709	1.5727
	SG-SVM	2.8219	1.9386	1.3997

# References

- [1] C. Wang, Z. Wang, J. Wang, and D. Zhao, "SVM-Based Parameter Identification for Composite ZIP and Electronic Load Modeling," IEEE Transactions on Power Systems, accepted for publication.
- [2] C. Wang, Z. Wang, J. Wang and D. Zhao, "Robust Time-Varying Parameter Identification for Composite Load Modeling," IEEE Transactions on Smart Grid. accepted for publication.
- [3] Introduction to WECC Modeling and Validation Work Group, WECC, March 24, 2018.
- [4] Load Model Complexity Analysis and Real-Time Load Tracking, PSERC, March 2017.
- [5] The New Aggregated Distributed Energy Resources (*der\_a*) Model for Transmission Planning Studies, EPRI, April, 2018.
- [6] CMPLDWG Composite Model with Distributed Generation DER\_A, California ISO, May, 2018.
- [7] Dmitry Kosterev, Anatoliy Meklin, John Undrill, Bernard Lesieutre, William Price, David Chassin, Richard Bravo, and Steve Yang. Load modeling in power system studies: WECC progress update. In Proc. IEEE PES Gen. Meet., Jul. 2008.
- [8] Alex Borden and Bernard Lesieutre. Model validation: FIDVR event. Technical report, University of Wisconsin-Madison, Madison, WI, 2009.
- [9] Q. Huang, R. Huang, B. J. Palmer, Y. Liu, S. Jin, R., Y. Chen and Y. Zhang, "A Reference Implementation of WECC Composite Load Model in Matlab and GridPACK." arXiv preprint arXiv:1708.00939, 2017.
- [10] WECC Dynamic Composite Load Model (CMPLDW) Specifications, January 27, 2015.
- [11] L. Luo and S. V. Dhople, "Spatiotemporal model reduction of inverter based islanded microgrids," IEEE Trans. Energy Convers., vol. 29, no. 4, pp. 823–832, Dec. 2014.



Thank you!

Q&A

Zhaoyu Wang  
<http://wzy.ece.iastate.edu/>